**Research article**

# Research on energy-saving factors adaptability of exterior envelopes of university teaching-office buildings under different climates (China) based on orthogonal design and EnergyPlus

Zu'an Liu [a,1], Jiawen Hou [a,1,*], Lili Zhang [b], Bart Julien Dewancker [a], Xi Meng [c], Chaoping Hou [b]

[a] *Faculty of Environmental Engineering, The University of Kitakyushu, Fukuoka, 808-0135, Japan*
[b] *College of Architecture and Urban-Rural Planning, Sichuan Agricultural University, Dujiangyan, 611830, China*
[c] *Innovation Institute for Sustainable Maritime Architecture Research and Technology, Qingdao University of Technology, Qingdao, 266033, China*

## ARTICLE INFO

## ABSTRACT

To achieve carbon neutrality in 2060 (China), building energy-saving has been highly concerned. University buildings have great energy-saving potential as part of energy consumption where 70% of energy loss is caused by heat transfer from the envelope. However, most of the research on energy-saving factors for envelopes is limited to a certain climate or a specific building type, and the optimal configuration of envelopes under different climatic regions has not been well solved. Therefore, the influence degree and appropriate parameters of each factor of the teaching-office building envelopes on energy consumption under different climates were analyzed in this paper by orthogonal design and numerical simulation. Results show that: (1) Solar heat gain coefficient ($SHGC$) and indoor air change rates ($ACH$) [the heat transfer coefficient of the exterior wall ($K_{wall}$) and $ACH$] are the main factors affecting the cooling [heating] load, the insulation form of the exterior wall ($W_{ins}$) and $K_{wall}$ [$W_{ins}$ and solar radiation absorption coefficient of exterior surface materials ($\rho_s$)] have less influence; (2) The important ranking and optimal level of the influence of each factor on the cooling (or heating) loads are related to local load demands; (3) For the annual load, $K_{wall}$ and the heat transfer coefficient of the exterior window ($K_{win}$) is the focus of energy-saving in severe cold and cold zones, but their impact is not significant in Guangzhou and Kunming, and the high significance of $SHGC$ is only shown in Hohhot, Lhasa, Guangzhou, and Haikou; (4) The annual load energy savings reach 39.64%–57.57% in different climates by optimizing all factors. The research results can provide directions and data references for the energy-saving design and renovation of educational building envelopes in different climates (China).

## 1. Introduction

Energy scarcity has caused great concern in the context of China's rapid economic development. According to statistics [1], China's building energy consumption shows a continuous growth in both public and residential buildings, the total energy consumption has increased from 10% in the late 1970s to over 30% now [2]. However, university buildings as a kind of public building, their energy consumption accounts for 31% of society and 84.1% of universities of the total energy consumption [3], so its energy-saving must be highly focused to achieve the 2060 carbon neutrality target. Meanwhile, its educational environment is also improving with the state's investment in higher education construction. Air-conditioning and heating equipment began to be installed in all

teaching-office buildings to improve indoor comfort and ensure the learning efficiency and teaching quality of students and teachers, which also lead to higher energy consumption. Therefore, many scholars have put a lot of efforts into research on active and passive building strategies to ensure indoor thermal comfort while reducing energy consumption in building operations [4, 5, 6]. Active strategies are mainly concentrated on some mechanical equipment, such as heating, ventilation and air conditioning systems, boilers and lighting. However, active technologies usually face the problem of relatively low energy efficiency of the equipment. Therefore, the research and application of passive technologies have received extensive attention [7, 8]. The main ones include, adding Trombe walls [9, 10, 11], lightweight concrete walls [12, 13], insulation materials [14], phase-change materials [15, 16, 17],

---

retro-reflective materials [18] and green roofs [19, 20]. The main purpose is to reduce the heat exchange between outdoor and indoor environments by improving the thermal performance of the building envelope, to obtain high thermal comfort and building energy savings. But for different outdoor environments or indoor thermal requirements, both excessive heat gain and insulation will harm the energy-saving on the cooling or heating load [21]. It further illustrates that the thermal performance of the building envelope significantly affects the indoor thermal environment and energy efficiency [21, 22, 23]. Balaras et al. [24] pointed out that the insulated buildings may consume 20%–40% less energy than non-insulated buildings in Greece, while Zhang et al. [14] found by DeST (Designer's Simulation Toolkit) that the increase in insulation can significantly reduce the heating load but results in an increase in summer cooling load. Semprini et al. [25] discovered by measuring different classroom micro-climates in a typical historic building at the University of Bologna (Italy) that the uncontrollable indoor thermal environment due to poor insulation of envelopes, while potential energy savings of up to 32% can be achieved by retrofitting the building with less impactful materials. Charles et al. [26] used SIMEB to simulate the effects of different exterior walls, roofs, windows and airtightness on building energy consumption concluding that increasing wall insulation, replacing windows and so on, could reduce the annual total energy consumption by 45%.

As a result, more and more researchers and engineers have realized that the energy-saving performance of buildings can be improved by improving the envelope configuration. Braulio-Gonzalo [27] and Hou et al. [28] optimized the thickness of the insulation material by utilizing an economic evaluation to balance the demand and cost of the building environment. Yu et al. [29] conducted an energy simulation of three exterior wall insulation systems by using DesignBuilder and pointed out that the insulation effect was not only related to the insulation thickness but also the insulation form. Thus, Leccese et al. [30] demonstrated the effect of continuous changes in the location and thickness distribution of the insulation material on the dynamic thermal performance (dynamic thermal transmittance, attenuation coefficient and delay time) by applying an analytical model based on the heat transfer matrix. In addition, it can also be observed by previous studies [31, 32, 33] that numerical simulation has become a widely used method to optimize the energy-saving of building envelopes. However, Huang and Niu [34] criticized in a literature review that a number of previous studies on simulation-based building envelope optimization used a single factor for the energy-saving optimization solutions. Actually, for the actual building, several variables or factors are usually involved [35]. For example, the wall of insulation form [36, 37, 38] and the heat transfer coefficient [39], the window-to-wall ratio and the type of glazing [21, 35], and so on. Meanwhile, Košir et al. [40] evaluated the effect of different thermal absorption rates of exterior surface materials on building energy consumption in different climate zones and discovered that it has a significant effect, and there was more energy-saving to use cold coatings for exterior surfaces with hot and dry conditions and poor insulation in building envelopes. Zhou et al. [41] found that the difference in air-conditioning energy consumption increased nearly twofold due to different climates by simulating the energy consumption of different combinations of three key influencing factors (climate, building envelope, and occupant behavior) for office buildings in four regions (Beijing, Taiwan, Hong Kong, and Berkeley).

In addition, the area of the exterior windows usually exceeds 20% that exterior walls and even more than 50% for university buildings, meanwhile, the heat transfer coefficient of exterior windows is usually more than four times that of exterior walls [42]. Therefore, exterior windows as another component of the envelope are also the key to energy-saving research. Capeluto and Ochoa [35] identified and ranked preferred configurations of energy-saving retrofit solutions for building envelopes for 13 central cities in European through numerical simulations, and found that insulation and glazing properties had a substantial influence on reducing energy consumption. Pan et al. [43] combined

with DeST to conduct an orthogonal design on the heat transfer coefficients of exterior walls ($K_{wall}$) and windows ($K_{win}$) and the shading coefficients of exterior windows ($SC_{win}$) for the Shanghai building. The results showed that the important order affecting the cooling load was $SC_{win} > K_{win} > K_{wall}$, affecting the heating load was $K_{wall} > SC_{win} > K_{win}$ and the annual load was $SC_{win} > K_{win} > K_{wall}$, which means that the thermal performance of exterior windows has different effects on energy-saving in different seasons. Besides, Lyu et al. [44] proposed a new triple insulating glass-water flow window and revealed that the heat gained from the window can be reduced by 43%, 44%, and 42% in the cold zone (CZ), hot summer and cold winter (HSCW) and hot summer and warm winter (HSWW) by numerical simulations. Aburas et al. [45] reviewed thermochromic films, coatings and glazing materials and found that the energy-saving potential of thermochromic glass can reach 5.0%–84.7% in heating and cooling under different climatic conditions. As a result, it can be concluded that the building envelope being improved can effectively increase energy-saving. But the influence degree of each factor of the envelope, optimized values and the energy-saving potential are very different in different climatic zones [41, 46, 47, 48].

In the meantime, we can discover based on the above studies whether add Trombe walls [9, 10, 11, 49] and insulation materials [8, 14] for non-transparent envelopes (exterior walls or roofs) or replace high-performance transparent envelopes (exterior windows) [35, 40, 44, 45], which all were designed to achieve indoor thermal comfort and energy saving by improving the thermal performance (or parameters) of the envelope, but all were limited to a single factor. Followed by most of the research on energy-saving strategies for envelopes was limited to a certain climate or a specific building type and the optimal configuration of envelopes under different climatic regions has not been well solved. Thus, to investigate the influence of multiple factors on the energy saving of the university teaching-office building exterior envelope, we have summarized the energy-saving factors affecting the thermal performance of the envelope in previous literature. The major factors include the heat transfer coefficients of external walls ($K_{wall}$) and windows ($K_{win}$) [25, 26, 39, 43, 48], and the form of insulation ($W_{ins}$) [36, 37, 38], the solar radiation absorption coefficient ($\rho_s$) of the external surface material [18, 40], the heat gain of the external windows ($SHGC$) and the indoor air change rate ($ACH$) [42, 43, 45]. It is apparent that the optimal designs of the building envelope with energy simulation technologies require multi-factor analysis under the differences in climate and thermal comfort requirements [21]. However, based on the existing research, it is worthwhile to explore the following issues:

- How do ensure the accuracy of numerical models and the validity of results for the optimal design of building envelopes?
- How do design fractional factorial experiments to cover the important features of the problem understudied?
- How do derive optimal solutions for exterior envelopes in different climates and multi-factorial analysis?

Hence, it is necessary to develop a highly efficient approach to deal with the optimization of multiple factors with different levels of value. Orthogonal experimental design as an important mathematical method, aiming to identify the representative cases for lowering the number of test cases [21, 50]. A more accurate and reliable optimization conclusion can be obtained with a fewer number of experiments after using an orthogonal design, and it allows for performing both range analysis (R) and analysis of variance (ANOVA) to evaluate test results. There is growing interest in the use of orthogonal design methods for optimization in various fields [28, 51, 52, 53, 54, 55]. Therefore, a university teaching-office building was researched in this paper through orthogonal design and numerical simulation (EnergyPlus) to explore the adaptability (including the optimal parameters and influence degree of each factor of the envelope and the significance levels) of the energy-saving factor of the building envelopes under different climates, which aims to provide the optimal solution for the renovation of university teaching-office

building envelopes under different climatic conditions in China to achieve maximum energy-saving building operations.

## 2. Methodology

### 2.1. Determination of climate zones and typical cities

As a country with diverse climate characteristics to ensure the basic indoor thermal environment and meet the national energy-saving, China has carried out climate zoning according to the need for building thermal design. The average temperature of the coldest month and the hottest month as the main indicators of zoning, and the number of days with an average temperature of not more than 5 °C and not less than 25 °C are used as auxiliary indicators (see Table 1), China is divided into five climate zones as shown in Figure 1, namely, severe cold zone (SCZ), cold zone (CZ), hot summer and cold winter zone (HSCW), hot summer and warm winter zone (HSWW), and moderate climate zone (MCZ) [56, 57]. To explore the energy-saving level of building envelope under different climatic conditions, the meteorological parameters of 12 typical cities in China are selected in this paper as the outdoor thermal boundary conditions of numerical simulation (it was downloaded from EnergyPlus official website [58]) according to the differences in topography, climate and culture, and their details are depicted in Figure1 and Figure 2. It can be observed a clear difference in climate characteristics of the different cities even if they belong to the same thermal zone, which further concludes that the cities selected in this paper are representative and the research results have certain guiding significance for building energy savings in most zones of China.

### 2.2. Case building description

A typical university teaching-office building was selected as the research object. It is located on the campus of Sichuan Agricultural University, 30 km northwest of Chengdu, China. The case building is a 5-story with a floor height of 3.9m, divided into three zones A, B, and C (three zones are relatively independent) with a total building area is 12,340m$^2$. Of these, zone A is fully used as classrooms, zone B floors 1–3 are offices and laboratories, 4–5 are painting studios and staff rooms, zone C 1–2 are meeting rooms, floors 3 are offices, floors 4–5 are offices and classrooms. The building plan is given in Figure 3. The thermophysical properties of the materials related to the building envelopes are given in Table 2 [56] and the construction methods and heat transfer coefficients of the main exterior envelope are shown in Table 3.

In addition, Chengdu as a typical city in HSCW, its hourly temperature and solar radiation intensity are presented in Figure 4 can be seen that the annual temperature is moderately between -2-28 °C and the climate is mild. The highest temperature is higher from June to August at around 30 °C and extreme weather may be above 35 °C. The minimum temperature is basically above 0 °C from December to February of the

following year, and extreme weather below 0 °C may occur. At the same time, the summer in Chengdu is longer than the wintertime, and the requirement for indoor cooling is higher than the heating requirement. However, considering the daily minimum temperature and the comfortable temperature of the human body, there is still a large heating demand in winter [14].

### 2.3. Orthogonal design

As mentioned earlier, orthogonal experimental design is an important mathematical method for the analysis of a specified target based on a multi-factor system and it is designed to be based on tabular forms with random errors for interaction among multiple factors and indicators, which is an efficient, fast and economical arrangement for experimental factors [43]. This step aims to analyze the effects of envelope-related parameters on building energy consumption and their energy-saving potential. Orthogonal design is used to arrange and test the performance of the proposed optimization strategies and further explore the feasible region of the energy optimization problem. The orthogonal table is the foundation of the orthogonal experimental design, it can be found in related books [60], which forms as follows:

$$L_D(Q^M) \tag{1}$$

Where $L$ represents the symbol of orthogonal design, $D$ denotes the number of rows or tests, $Q$ indicates the number of levels, and $M$ represents the number of columns or factors [21, 61].

The results of the orthogonal design are usually analyzed by the analysis of range (R) and analysis of variance (ANOVA). The range analysis aims to measure and demonstrate the impact range of each factor using the difference between the maximum and minimum mean values of test results. The results can be further analyzed through the ANOVA to identify the effects of experimental conditions, errors, and the importance of factors. For the statistics of the F-value distribution ($F_v$), the value of $F_v$ is compared to a critical value of a significant level, which is normally set at 0.05 or 0.01 [21,49,60]. The impact of the selected factor on the test results is considered to be significant if it is greater than the critical value, and vice versa.

Setting $x_k$ as the output result generated by the $k^{th}$ orthogonal test, the square sum of the total deviation ($S_T$) and the degrees of the total freedom ($df_T$), can be expressed as Eqs. (2) and (3). Herein, for the $m^{th}$ factor, the square sum of the deviation ($S_m$) and the freedom degrees ($df_m$), are expressed as Eqs. (4) and (5).

$$S_T = \sum_{k=1}^{n} x_k^2 - \frac{1}{D}\left(\sum_{k=1}^{D} x_k\right)^2 \tag{2}$$

$$df_T = D - 1 \tag{3}$$

$$S_m = \frac{1}{D/Q}\sum_{i=1}^{Q} D_{i,m}^2 - \frac{1}{D}\left(\sum_{k=1}^{D} x_k\right)^2 \tag{4}$$

$$df_m = Q - 1 \tag{5}$$

For errors, the square sum of the deviation ($S_e$), and the freedom degrees ($df_e$), are defined as Eqs. (6) and (7).

$$S_e = S_T - \sum dS_m \tag{6}$$

$$df_e = f_T - \sum df_m \tag{7}$$

The F-value ($F_v$) of each factor can be calculated by Eq. (8).
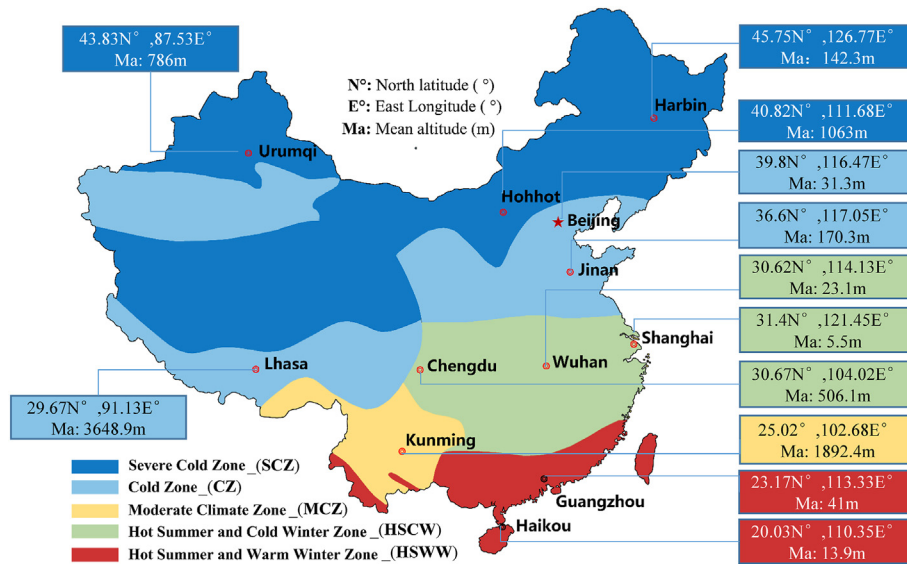
$$F_v = \frac{MS_m}{MS_e} \tag{8}$$

**Table 1.** Summary of climate classification criteria [56, 57].

| Climate zone | Main criteria | Complementary criteria |
|---|---|---|
| Severe cold zone (SCZ) | ATCM ≤ -10 °C | 145 ≤ NDAT<5 |
| Cold zone (CZ) | -10 °C < ATCM ≤ 0 °C | 90 ≤ NDAT5 < 145 |
| Hot summer and cold winter zone (HSCW) | 0 °C < ATCM ≤10 °C<br>25 °C < ATHM ≤30 °C | 0 ≤ NDAT5 < 90<br>40 ≤ NDAT25 < 110 |
| Hot summer and warm winter zone (HSWW) | 10 °C < ATCM<br>25 °C < ATHM ≤29 °C | 100 ≤ NDAT25 < 200 |
| Moderate climate zone (MCZ) | 0 °C < ATCM ≤13 °C<br>18 °C < ATHM ≤25 °C | 0 ≤ NDAT5 < 90 |

ATCM = Average temperature in the coldest month; ATHM = Average temperature in the hottest month; NDAT5 = Number of days that average temperature is below 5 °C; NDAT25 = Number of days that average temperature is above 25 °C.

**Figure 1.** China's climate zones and 12 typical city location maps [56, 57].
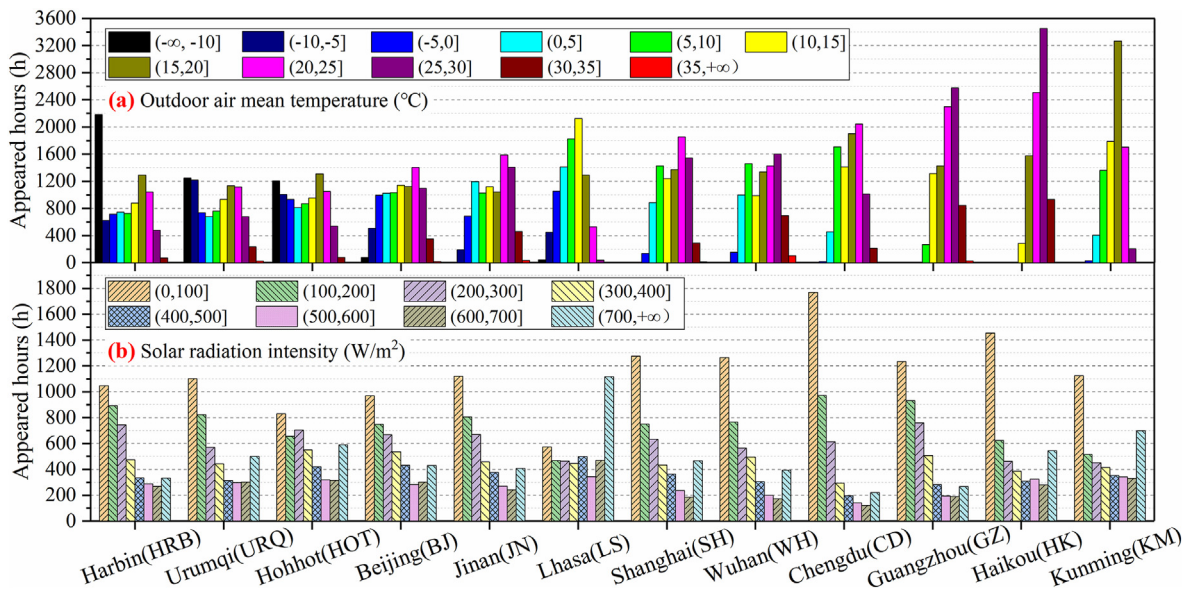


**Figure 2.** 12 typical cities (a) appeared hours of different outdoor temperature ranges and (b) appeared hours of different solar radiation intensity ranges [58, 59].

Six factors are selected in this paper to characterize the thermal performance of the building envelope, each factor contains five levels, so the orthogonal design table $L_{25}$ ($5^6$) is used for the design as presented in Table 4. The six factors are $A$-the insulation form of the exterior wall ($W_{ins}$), $B$- the heat transfer coefficient of the exterior wall ($K_{wall}$), $C$- wall exterior surface material solar radiation absorption coefficient ($\rho_s$), $D$-the solar heat gain coefficient of exterior window ($SHGC$), $E$-the heat transfer coefficient of the exterior window ($K_{win}$) and $F$- air change rate per hours ($ACH$), whose thermal performance indexes accurately demonstrate the thermal insulation and airtightness of the building envelope. Table 5 lists the level values of the above factors based on the "code for thermal design of civil building" [56].

### 2.4. Energy simulation

#### 2.4.1. EnergyPlus

EnergyPlus is a building energy time-to-time simulation software developed by the U.S. Department of Energy (DOE) and Lawrence Berkeley National Laboratory (LBNL) based on BLAST and DOE-2, which applies an integrated and synchronized load/system/equipment simulation method [62]. The loads and room temperatures are calculated by using the heat balance method, the envelope heat transfer is determined by the conduction transfer functions (CTF) [63] and the airflow between zones is simulated by defining the flow rate and time or COMIS modules [64]. Moreover, the WINDOWS program [65] is used to calculate the heat transfer from exterior windows and the solar heat gain from the glazing. EnergyPlus calculations have high accuracy and are mainly used to predict building energy consumption, and their simulation results have been validated in numerous analytical, comparative, and empirical cases [49].

The computational process of EnergyPlus is based on the integrated processing of multi-program modules [65, 66] whose core is the basic heat balance principle, it can be simplified as Eq. (9) [21, 28].

$$\sum_{i=1}^{N_{sl}} \dot{Q}_i + \sum_{i=1}^{N_{surfaces}} h_i A_i (T_{si} - T_z) + \sum_{i=1}^{N_{zones}} \dot{m}_i C_p (T_{zi} - T_z) + \dot{m}_{inf} C_p (T_\infty - T_z) + \dot{Q}_{sys} = 0$$

(9)

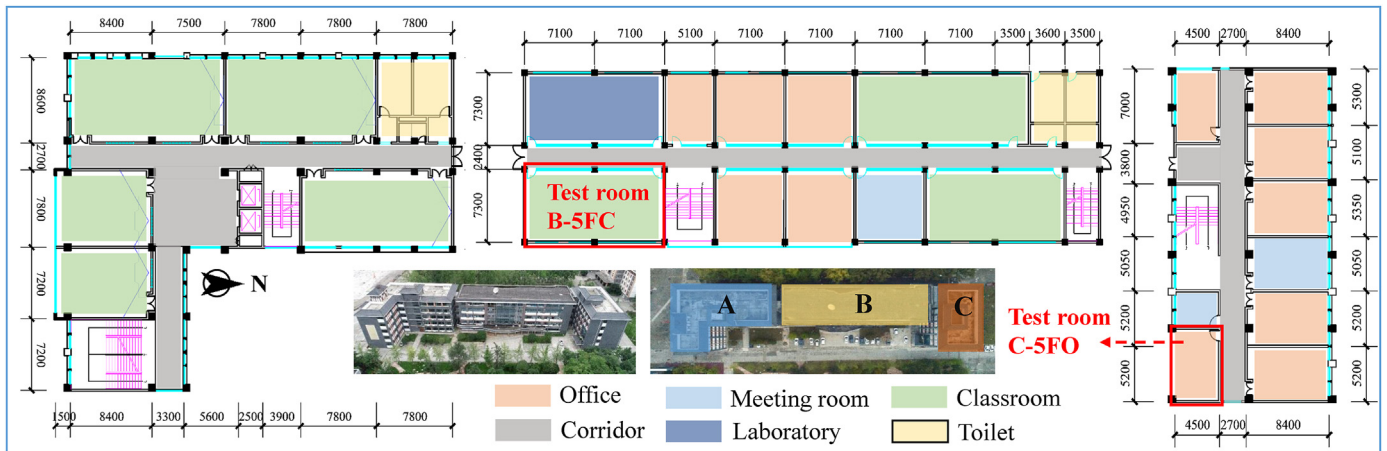**Figure 3.** Building plane diagram.

**Table 2.** Thermophysical parameters of the building envelopes.

| Materials | Thermal conductivity, $\lambda$ (W/m·K) | Specific heat, $c$ (kJ/kg·K) | Density, $\rho$ (kg/m³) |
|---|---|---|---|
| Facing brick | 2.03 | 0.92 | 2400 |
| Expanded pearlite | 0.06 | 0.67 | 120 |
| Cement mortar | 0.93 | 1.05 | 1800 |
| Gypsum mortar | 0.19 | 1.05 | 500 |
| Porous shale brick | 0.58 | 1.05 | 1400 |
| Extruded polystyrene (XPS) | 0.03 | 1.38 | 35 |
| Plywood | 0.17 | 2.51 | 600 |
| Aluminium alloy | 203 | 0.92 | 2720 |
| Asphalt waterproof | 0.17 | 1.47 | 600 |
| Boiler slag | 0.29 | 0.92 | 1000 |
| Reinforced concrete | 1.74 | 0.92 | 2500 |
| Lime mortar | 0.87 | 1.05 | 1700 |
| Ceiling tile | 0.33 | 1.05 | 1050 |
| Air layer | Thermal resistance, 0.18 [(m²·K)/W] | | |
| Plain concrete | 0.52 | 0.98 | 1300 |

**Table 3.** The construction method and heat transfer coefficient of main external envelope.

| Building envelopes | Thickness and material of each layer from outside to inside | Heat transfer coefficient, $k$ [W/(m²·K)] |
|---|---|---|
| Exterior wall | 8 mm Facing brick +20 mm Cement mortar +20 mm Expanded pearlite +200 mm Porous shale brick +20 mm Lime mortar + Facing layer | 0.984 |
| Roof | 25 mm Cement mortar +45 mm XPS+6 mm Asphalt waterproof +20 mm Cement mortar +30 mm Boiler slag +120 mm Reinforced concrete + Air layer +10 mm Ceiling tile | 0.526 |
| Exterior window | Heat breaking aluminum alloy ordinary hollow glass (6 + 12A + 6) | 3.40 |
| Interior wall | 2mm Gypsum mortar +20 mm Cement mortar +200 mm Porous shale brick +20 mm Cement mortar + 2mm Gypsum mortar | 2.45 |
| Door | 0.8mm Aluminium alloy +30mm Plywood+0.8mm Aluminium alloy | 5.67 |
| Interior window | Heat breaking aluminum alloy ordinary hollow glass (6 + 12A + 6) | 3.40 |

In addition, the air heat balance in EnergyPlus can be formulated as Eqs. (10) and (11).

$$C_z \frac{dT_z}{dt} = \sum_{i=1}^{N_{sl}} \dot{Q}_i + \sum_{i=1}^{N_{surfaces}} h_i A_i (T_{si} - T_z) + \sum_{i=1}^{N_{zones}} \dot{m}_i C_p (T_{zi} - T_z) + \dot{m}_{inf} C_p (T_\infty - T_z) + \dot{Q}_{sys} \tag{10}$$

$$C_z = \rho_{air} C_p C_T \tag{11}$$

Where, $\sum_{i=1}^{N_{sl}} \dot{Q}_i$ represents the sum of the convective internal loads, J; $\sum_{i=1}^{N_{surfaces}} h_i A_i (T_{si} - T_z)$ represents the convective heat transfer from the zone surfaces, W; $m_{inf} C_p (T_\infty - T_z)$ represents heat transfer due to infiltration of outside air, J/s; $\sum_{i=1}^{N_{zones}} m_i C_p (T_{zi} - T_z)$ represents heat transfer due to interzone air mixing, J/s; $\dot{Q}_{sys}$ is air systems output, J; $C_z \frac{dT_z}{dt}$ represents energy stored in zone air, J/kg; $\rho_{air}$ is zone air density, kg/m³; $C_p$ is zone air specific heat, J/(kg·K); $C_T$ is sensible heat capacity multiplier, J/(kg·K).

### 2.4.2. Numerical modeling and validation

In the numerical modeling, SketchUp is used as the platform for geometric modeling using Openstudio plug-in based on the actual building drawings, site mapping data and the different room functions to establish the corresponding thermal zone. Meanwhile, the construction form of the exterior envelope and related thermal parameters are set by the actual data in section 2.2. Detailed data are shown in Table 2 and Table 3. Figure 5 shows the schematic diagram of the EnergyPlus numerical model.

To validate the accuracy of numerical models and the reliability of simulation results, two representative rooms in the case building were selected for testing in this paper, which is commonly used classroom (zone-B-5th Floor Classroom, B–5FC) and office (zone-C-5th Floor Office, C–5FO), the details location are displayed in Figure 3. The experimental tests were conducted from July 12 to July 22 and the test parameters mainly include outdoor solar radiation intensity, wind speed, indoor and outdoor air temperature, relative humidity. The measurement of temperature and relative humidity were located at 1.5 m high above the floor (the middle of the test room), and the outdoor parameters were arranged on the roof (no shade), which are shown in Figure 6. All tests were done according to the relevant standards [67] and data were recorded at 15
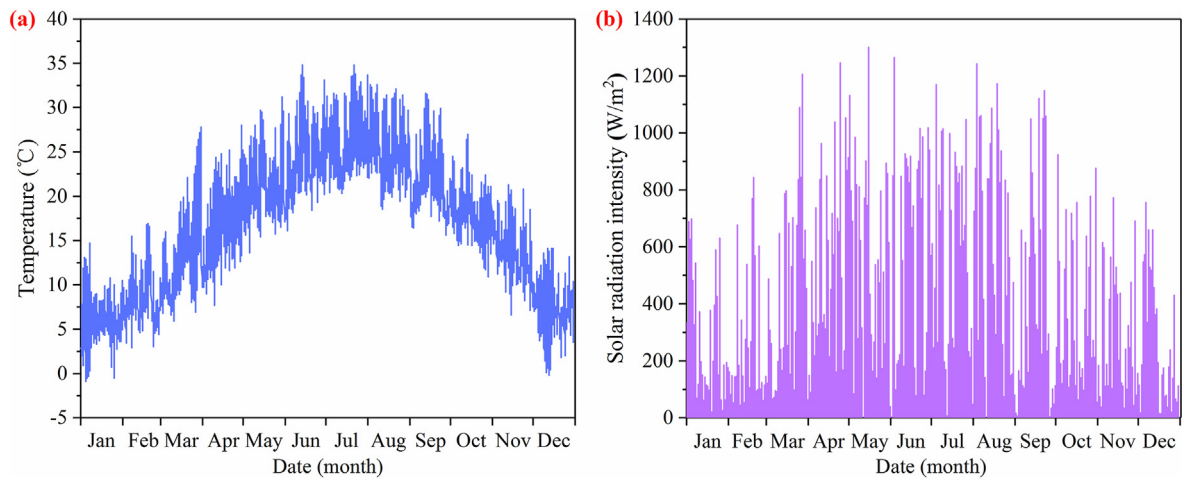
**Figure 4.** Chengdu climate condition: (a) annual hourly temperature, and (b) solar radiation intensity [14].

**Table 4.** Orthogonal experimental 'L$_{25}$ (5$^6$)' condition design.

| Experiment Number | A (W$_{ins}$, -) | B [K$_{wall}$, W/(m$^2$.K)] | C ($\rho_s$, -) | D (SHGC,-) | E [K$_{win}$, W/(m$^2$.K)] | F (ACH,1/hr) |
|---|---|---|---|---|---|---|
| 1 | 1 | 1 | 1 | 1 | 1 | 1 |
| 2 | 1 | 2 | 2 | 2 | 2 | 2 |
| 3 | 1 | 3 | 3 | 3 | 3 | 3 |
| 4 | 1 | 4 | 4 | 4 | 4 | 4 |
| 5 | 1 | 5 | 5 | 5 | 5 | 5 |
| 6 | 2 | 1 | 2 | 3 | 4 | 5 |
| 7 | 2 | 2 | 3 | 4 | 5 | 1 |
| 8 | 2 | 3 | 4 | 5 | 1 | 2 |
| 9 | 2 | 4 | 5 | 1 | 2 | 3 |
| 10 | 2 | 5 | 1 | 2 | 3 | 4 |
| 11 | 3 | 1 | 3 | 5 | 2 | 4 |
| 12 | 3 | 2 | 4 | 1 | 3 | 5 |
| 13 | 3 | 3 | 5 | 2 | 4 | 1 |
| 14 | 3 | 4 | 1 | 3 | 5 | 2 |
| 15 | 3 | 5 | 2 | 4 | 1 | 3 |
| 16 | 4 | 1 | 4 | 2 | 5 | 3 |
| 17 | 4 | 2 | 5 | 3 | 1 | 4 |
| 18 | 4 | 3 | 1 | 4 | 2 | 5 |
| 19 | 4 | 4 | 2 | 5 | 3 | 1 |
| 20 | 4 | 5 | 3 | 1 | 4 | 2 |
| 21 | 5 | 1 | 5 | 4 | 3 | 2 |
| 22 | 5 | 2 | 1 | 5 | 4 | 3 |
| 23 | 5 | 3 | 2 | 1 | 5 | 4 |
| 24 | 5 | 4 | 3 | 2 | 1 | 5 |
| 25 | 5 | 5 | 4 | 3 | 2 | 1 |

min intervals. Table 6 shows the accuracy and measurement range of the test instruments.

Considering the stability of the experimental instruments, the measured outdoor meteorological data (air temperature, air humidity, solar radiation intensity, wind speed) for 72 h continuously during the summer experimental test period from July 16 to July 18 were taken as the boundary conditions in this study. Figure 7 gives the comparison between the measured and simulated hourly air temperature in the test

**Table 5.** Five levels of every factor designed.

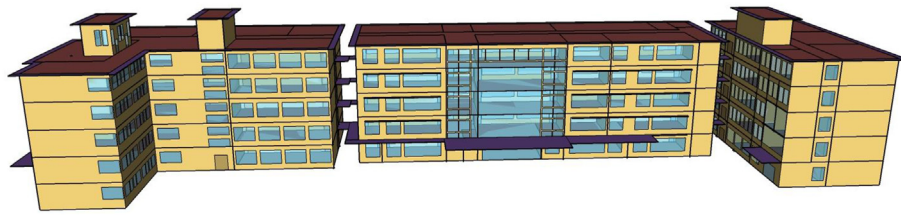| Levels | A (W$_{ins}$) | B(K$_{wall}$) | C ($\rho_s$) | D (SHGC) | E (K$_{win}$) | F (ACH) |
|---|---|---|---|---|---|---|
| 1 | Exterior insulation wall (E$_w$) | 0.2 | 0.15 | 0.35 | 1.5 | 0.5 |
| 2 | Interior insulation wall (I$_w$) | 0.4 | 0.45 | 0.45 | 2.5 | 1 |
| 3 | Sandwich insulation wall (S$_w$) | 0.6 | 0.55 | 0.55 | 3.5 | 1.5 |
| 4 | Lightweight self-insulation wall (L$_w$) | 0.8 | 0.65 | 0.65 | 4.5 | 2 |
| 5 | Heavyweight self-insulation wall (H$_w$) | 1.0 | 0.75 | 0.75 | 5.5 | 2.5 |

**Figure 5.** Numerical model constructed by EnergyPlus.
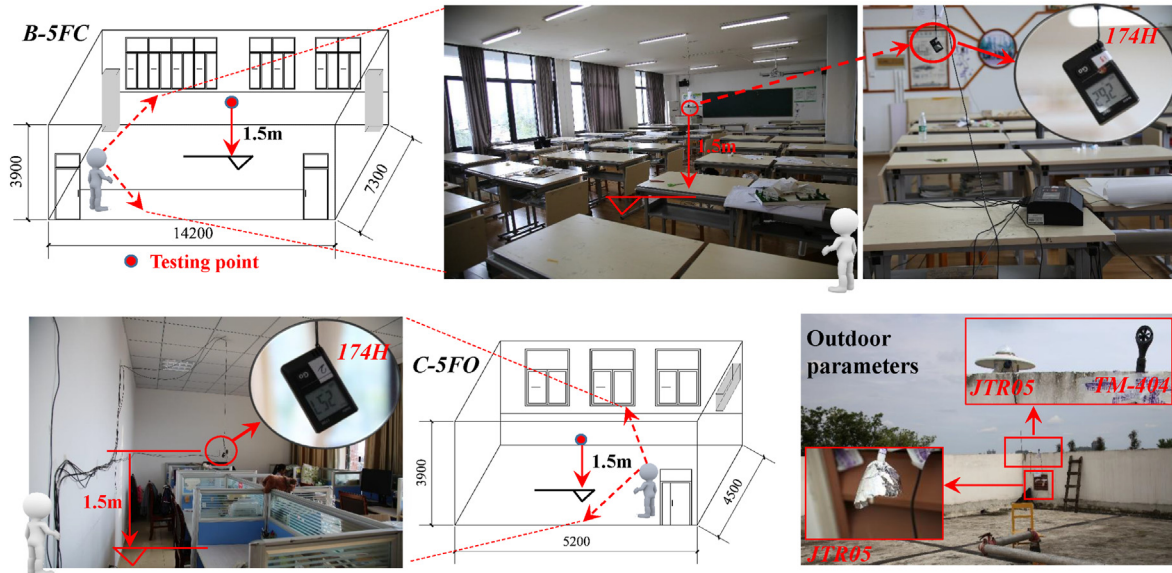


**Figure 6.** Layout of experimental testing points.

**Table 6.** Related parameters of experimental instruments.

| Test parameters | Picture | Brand and Model | Range | Accuracy | Resolution |
|---|---|---|---|---|---|
| Air temperature | | Testo, 174H-Mini | -20-70 °C | ±0.5 °C | 0.1 °C |
| Relative humidity | | | 0-100%RH | ±3%RH | 0.1%RH |
| Solar radiation intensity | | Jantytech, JTR05 | 0–2000W/m² | ±2% | 1W/m² |
| Air temperature | | | -50°C–50 °C | ±0.5 °C | 0.1 °C |
| Wind speed | | Tenmars, TM-404 | 0–25 m/s | ±2% + 0.2 | 0.1 m/s |

rooms B–5FC and C–5FO. To ensure the validation accuracy, two metrics: root mean square error (RMSE) and coefficient of variation (CV$_{(RMSE)}$) were employed [15, 68, 69], while RMSE measures the average spread of errors which provided a measure for the model's dispersion [68, 70], CV$_{(RMSE)}$ is the coefficient of variation in RMSE, as expressed by Eqs. (12) and (13), respectively, as follows:

$$RMSE = \sqrt{\frac{1}{n} \sum_{t=1}^{n} (M_t - S_t)^2} \qquad (12)$$

$$CV_{(RMSE)} = \frac{RMSE}{\overline{M_t}} \times 100\% \qquad (13)$$

It is found by calculation that the RMSE of the present numerical results is only 0.38 °C and 0.37 °C respectively for B–5FC and C–5FO, compared to experimental results, and the CV$_{(RMSE)}$ are same only 1.37%.
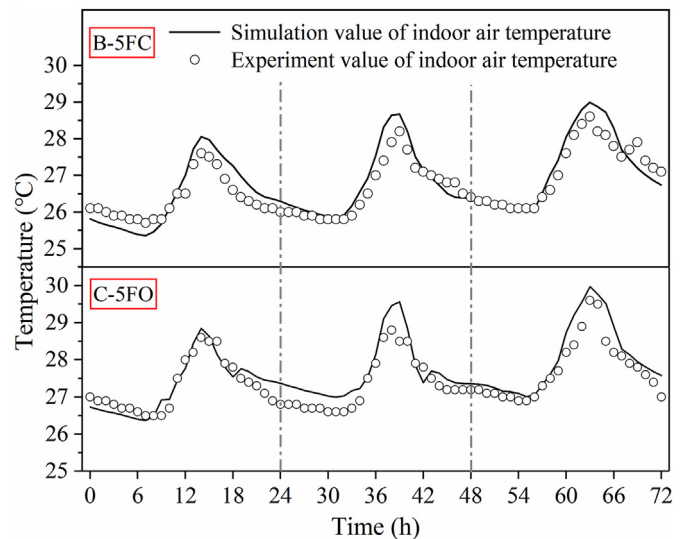


**Figure 7.** Comparison of numerical indoor air temperature with experimental results.

These results meet the simulation requirements with the ASHRAE criterion of CV$_{(RMSE)}$ less than 30% [71] and indicate the ability of EnergyPlus for predicting the targets in this study.

*2.4.3. Determination of the numerical model*

Only zone-C is chosen as the object of study considering the computational speed of numerical simulation. A schematic diagram of the wall
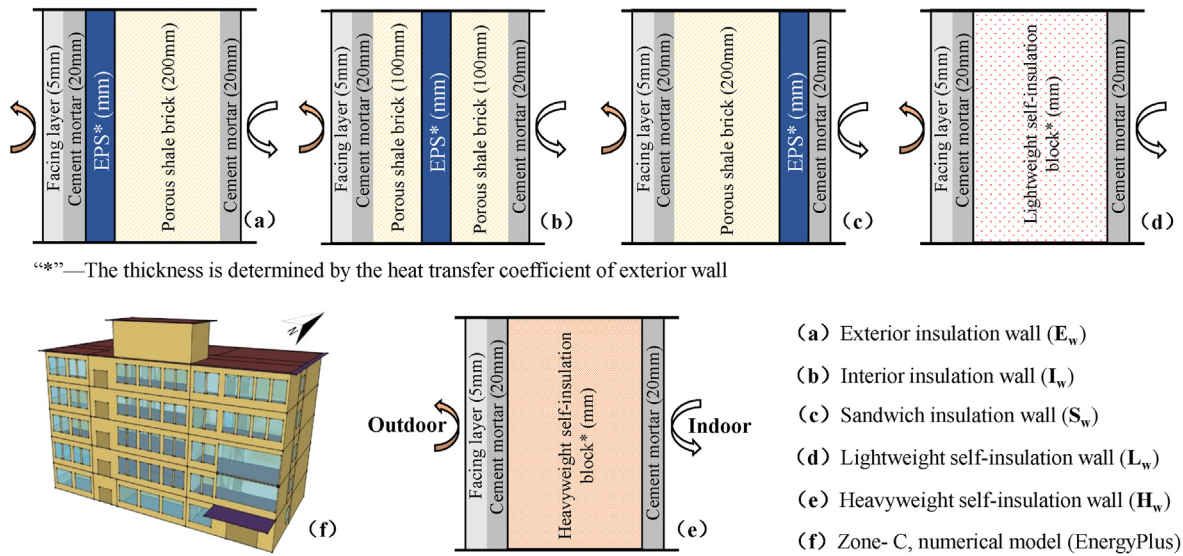
**Figure 8.** Wall insulation form and numerical simulation model (zone-C).

**Table 7.** Thermophysical parameters of wall materials.

| Material | Density, $\rho$(kg/m$^3$) | Specific heat capacity, $c$ (J/kg·K) | Thermal conductivity, $\lambda$(W/m·K) |
|---|---|---|---|
| Facing layer | 1500 | 1200 | 2.030 |
| Cement mortar | 1800 | 1050 | 0.930 |
| Porous shale brick | 1400 | 1050 | 0.580 |
| Expanded Polystyrene (EPS) | 20 | 1380 | 0.039 |
| Lightweight self-insulation block | 314 | 921 | 0.078 |
| Heavyweight self-insulation block | 1026 | 1298 | 0.078 |

insulation form and the zone-C numerical model are displayed in Figure 8, and the relevant thermophysical parameters of the calculation model are shown in Table 7. Moreover, considering the high personnel density of university teaching-office buildings, the office and classroom were set to 0.15 person/m$^2$ and 0.5 person/m$^2$, respectively, the power used for indoor lighting was set to 4 W/m$^2$ and the personnel activity (sitting and slight movement) was set at 72 W/person [72, 73].

Meanwhile, to simulate the air-conditioning load of university teaching-office buildings only the ideal air conditioning system was set up in offices and classrooms. Considering that Chinese universities have winter and summer vacations, the air conditioning operation cycle in summer was set from May 15 to July 15 with the temperature set at 26 °C, the temperature is set to 20 °C from November 15 to January 25 in winter. Air-conditioners run from 08:00–12:00, 14:00–18:00, and 19:30–22:00 every day. The meteorological data were selected for the simulation with CSWD (Chinese Standard Weather Data) format [58], which was derived from the "Specialized meteorological dataset for building thermal environment analysis in China" [59] developed by Tsinghua University and the China Meteorological Bureau. And the base

data is the actual measurement data from Chinese weather stations, which are more authoritative and reliable, so the simulation results are more informative for the building energy consumption in Chinese climate zones.

## 3. Results and discussion

### 3.1. Analysis of energy simulation results

#### 3.1.1. Energy simulation results for original buildings in different climates

Different climatic conditions not only determine the local demand for cooling and heating loads in buildings but also further influences the building energy-saving optimization objectives. Therefore, Table 8 gives the proportion of cooling and heating loads in the whole year (8760h) of buildings with the same thermal performance under different climatic conditions. The demand for cooling and heating loads varies greatly in different climate zones or cities. The heating load in Harbin (SCZ) accounts for 94.6% of the total load under the same building thermal performance, while it can be ignored in Haikou (HSWW). In terms of total annual load, the SCZ is the focus of energy-saving, being 8 times higher than the Kunming (MCZ) where the load demand is lower. Moreover, the cooling and heating loads under the same thermal zone are also different due to the differences in geographical location, altitude, solar radiation intensity and sunshine hours between cities. Taking CZ as an example, the cooling load demand of Jinan is 38.2% higher than that of Beijing when the total load difference between Beijing and Jinan is small, while the heating load is 18.9% lower. At the same time, the cooling load demand in Lhasa is reduced by 87.7% and 91.1% compared to Beijing and Jinan, and the heating load is reduced by 46.3% and 33.8%, respectively. The above data are sufficient to demonstrate the importance of energy-saving design according to different climatic conditions and different cooling and heating load requirements.

**Table 8.** Energy simulation results for the original building (Zone-C) in different climates/cities.

| Climate zone | SCZ | | | CZ | | | HSCW | | | HSWW | | MCZ |
|---|---|---|---|---|---|---|---|---|---|---|---|---|
| City | HRB | URQ | HOT | BJ | JN | LS | SH | WH | CD | GZ | HK | KM |
| Cooling load (kWh/m$^2$) | 5.79 | 9.52 | 8.8 | 16.05 | 22.18 | 1.97 | 18.57 | 24.11 | 16.58 | 42.69 | 56.88 | 9.38 |
| Heating load (kWh/m$^2$) | 101.78 | 75.63 | 69.39 | 41.46 | 33.61 | 22.25 | 15.39 | 17.95 | 16.40 | 0.35 | 0.01 | 4.46 |
| Total load (kWh/m$^2$) | 107.57 | 85.15 | 78.19 | 57.51 | 55.79 | 24.22 | 33.96 | 42.06 | 32.98 | 43.04 | 56.89 | 13.84 |

### 3.1.2. Energy simulation results for each typical city based on orthogonal design

To study the influence of the thermal performance of building envelope on cooling and heating load in different regions, the cooling, heating and total load of 12 typical cities in China are simulated and compared based on orthogonal design. Taking Chengdu as an example, the loads vary widely under different combinations of thermal performance of the exterior envelope based on the results of the orthogonal design in Table 9. The orthogonal combinations with the lowest cooling load (CL), heating load (HL) and total load (TL) are E12, E1 and E1, separately for Chengdu, and the energy-saving rate can reach 59.11%, 79.54% and 64.15% respectively compared with the highest load in other combinations. Also, the energy-saving rates of cooling, heating and total load can reach 64.1%, 55.9% and 51.2%, respectively compared with the original building load (see Table 8). It shows that the effect of different thermal properties of the envelope on the loads is extremely significant. In addition, Figure 9 gives the load values of 12 typical cities in different climatic zones under different orthogonal combinations, from which it can be seen that the cooling and heating loads vary greatly even if they belong to the same thermal zone or city due to differences in exterior envelope. The most pronounced performance is in the SCZ region, among all cities (SCZ), the optimal combinations are E1 in both heating load and total load mainly due to the heating load accounts for 80.56%–98.7% of the total load. Compared with the worst combination of E5, the heating and total load energy savings can reach 67.1%–69.1% and 64.9%–66.6%, and E1 energy saves can also reach more than 50% compared to the original building. However, for the Kunming (MCZ), the difference in the energy-saving effect of the envelope retrofit is small due to the low local demand for cooling and heating loads, but the optimal combination (E1) still reduces the total load by 77.7% compared to the worst combination (E13) and saving 65.0% compared to the original construction.

Meanwhile, cooling (E12) or heating (E1) under different demands can essentially achieve 100% energy savings with different envelope optimization designs. Furthermore, for HSWW with high cooling load demand (82.94%–100% of the total load), Guangzhou and Haikou can achieve 51.8% and 49.8% energy savings in cooling load and total load compared to the original building after optimization (E1). It can also be noted that the worst combination (E5) still results in 10.8% and 15.2% energy savings compared to the original building's total load. Again, it can also be concluded from the other climate zones (CZ, HSCW) that there are optimal parameters (or combinations) for the exterior envelope, and its optimal values are closely related to the local demand for cooling and heating. In summary, it is adequate to explain that the appropriate envelope parameters are different for different climatic zones (or cities) and that the importance of energy-saving renovation (or design) of building envelopes according to different regions cannot be overstated.

### 3.2. Influence degree and optimal value of each factor on load in different climatic zones

Based on the above analysis, the different thermal performance of envelopes has different impacts on energy consumption in different climate zones, and their differences are quite large. Although the optimal level combinations of the cooling, heating and total load for each typical city for 25 trials in the orthogonal design can be intuitively derived from Figure 9, the result is not necessarily optimal for all possible level pairings ($5^6 = 15625$). To determine the influence degree of each factor on building load and better combination, the average target deviation ($K_{i,m}$) and range ($R$) are calculated under different levels of each city, and the influence degree and optimization level in different climate zones on each load are obtained in this paper, where a larger $R$ means a larger

**Table 9.** Orthogonal design arrangements and results (take Chengdu as an example).

| No. | Design Parameters | | | | | | Evaluation index (Chengdu) | | |
|---|---|---|---|---|---|---|---|---|---|
| | A | B | C | D | E | F | CL | HL | TL |
| E1 | 1 ($E_w$) | 1 (0.2) | 1 (0.15) | 1 (0.35) | 1 (1.5) | 1 (0.5) | 8.84 | 7.23 | 16.07 |
| E2 | 1 ($E_w$) | 2 (0.4) | 2 (0.45) | 2 (0.45) | 2 (2.5) | 2 (1.0) | 7.92 | 16.49 | 24.41 |
| E3 | 1 ($E_w$) | 3 (0.6) | 3 (0.55) | 3 (0.55) | 3 (3.5) | 3 (1.5) | 7.84 | 23.7 | 31.54 |
| E4 | 1 ($E_w$) | 4 (0.8) | 4 (0.65) | 4 (0.65) | 4 (4.5) | 4 (2.0) | 9.04 | 29.46 | 38.5 |
| E5 | 1 ($E_w$) | 5 (1.0) | 5 (0.75) | 5 (0.75) | 5 (5.5) | 5 (2.5) | 9.5 | 35.33 | 44.83 |
| E6 | 2 ($I_w$) | 1 (0.2) | 2 (0.45) | 3 (0.55) | 4 (4.5) | 5 (2.5) | 8.16 | 32.78 | 40.94 |
| E7 | 2 ($I_w$) | 2 (0.4) | 3 (0.55) | 4 (0.65) | 5 (5.5) | 1 (0.5) | 11.48 | 11.2 | 22.68 |
| E8 | 2 ($I_w$) | 3 (0.6) | 4 (0.65) | 5 (0.75) | 1 (1.5) | 2 (1.0) | 14.55 | 12.28 | 26.83 |
| E9 | 2 ($I_w$) | 4 (0.8) | 5 (0.75) | 1 (0.35) | 2 (2.5) | 3 (1.5) | 6.69 | 23.94 | 30.63 |
| E10 | 2 ($I_w$) | 5 (1.0) | 1 (0.15) | 2 (0.45) | 3 (3.5) | 4 (2.0) | 6.11 | 30.25 | 36.36 |
| E11 | 3 ($S_w$) | 1 (0.2) | 3 (0.55) | 5 (0.75) | 2 (2.5) | 4 (2.0) | 11.12 | 24.21 | 35.33 |
| E12 | 3 ($S_w$) | 2 (0.4) | 4 (0.65) | 1 (0.35) | 3 (3.5) | 5 (2.5) | 5.95 | 34.55 | 40.5 |
| E13 | 3 ($S_w$) | 3 (0.6) | 5 (0.75) | 2 (0.45) | 4 (4.5) | 1 (0.5) | 8.98 | 12.61 | 21.59 |
| E14 | 3 ($S_w$) | 4 (0.8) | 1 (0.15) | 3 (0.55) | 5 (5.5) | 2 (1.0) | 8.1 | 19.46 | 27.56 |
| E15 | 3 ($S_w$) | 5 (1.0) | 2 (0.45) | 4 (0.65) | 1 (1.5) | 3 (1.5) | 10.34 | 20.8 | 31.14 |
| E16 | 4 ($L_w$) | 1 (0.2) | 4 (0.65) | 2 (0.45) | 5 (5.5) | 3 (1.5) | 7.33 | 24.24 | 31.57 |
| E17 | 4 ($L_w$) | 2 (0.4) | 5 (0.75) | 3 (0.55) | 1 (1.5) | 4 (2.0) | 8.95 | 25.35 | 34.3 |
| E18 | 4 ($L_w$) | 3 (0.6) | 1 (0.15) | 4 (0.65) | 2 (2.5) | 5 (2.5) | 8.33 | 31.94 | 40.27 |
| E19 | 4 ($L_w$) | 4 (0.8) | 2 (0.45) | 5 (0.75) | 3 (3.5) | 1 (0.5) | 12.8 | 10.56 | 23.36 |
| E20 | 4 ($L_w$) | 5 (1.0) | 3 (0.55) | 1 (0.35) | 4 (4.5) | 2 (1.0) | 7.06 | 21.2 | 28.26 |
| E21 | 5 ($H_w$) | 1 (0.2) | 5 (0.75) | 4 (0.65) | 3 (3.5) | 2 (1.0) | 10.56 | 15.42 | 25.98 |
| E22 | 5 ($H_w$) | 2 (0.4) | 1 (0.15) | 5 (0.75) | 4 (4.5) | 3 (1.5) | 10.12 | 22.09 | 32.21 |
| E23 | 5 ($H_w$) | 3 (0.6) | 2 (0.45) | 1 (0.35) | 5 (5.5) | 4 (2.0) | 6.15 | 31.56 | 37.71 |
| E24 | 5 ($H_w$) | 4 (0.8) | 3 (0.55) | 2 (0.45) | 1 (1.5) | 5 (2.5) | 7.35 | 32.86 | 40.21 |
| E25 | 5 ($H_w$) | 5 (1.0) | 4 (0.65) | 3 (0.55) | 2 (2.5) | 1 (0.5) | 10.38 | 11.67 | 22.05 |

Note: CL = Cooling Load, kWh/m$^2$; HL = Heating Load, kWh/m$^2$; TL = Total Load, kWh/m$^2$.
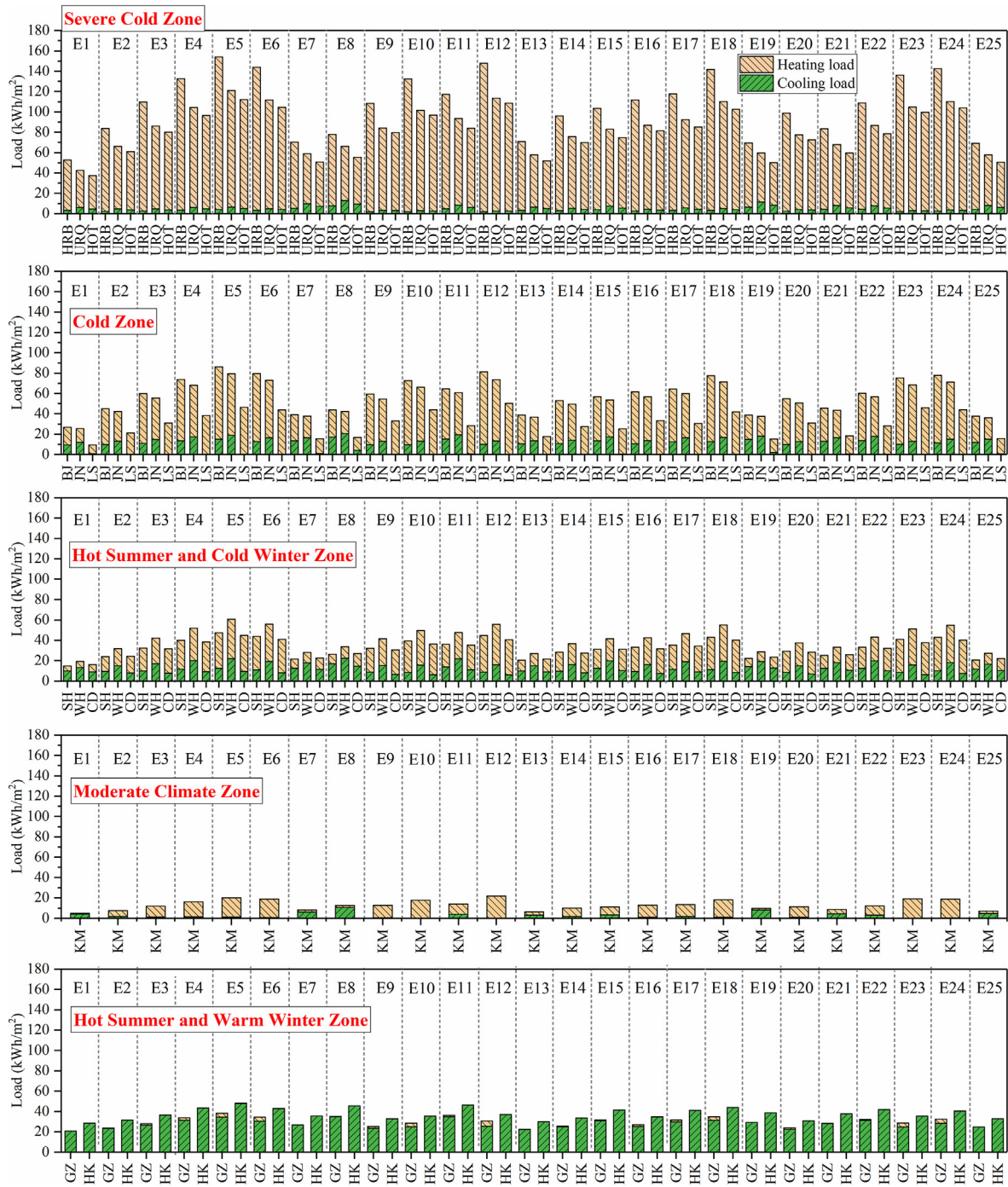
**Figure 9.** Cooling/heating loads for typical cities in different climates with different combinations of envelope parameters.

impact on the target, a lower $K_{i,m}$ shows a smaller load and means the corresponding parameter level is optimal for the target.

### 3.2.1. Influence degree of each factor

From Figure 10(a), it can be easily understood that the differences in the importance ordering of the various factor of the envelope on the influence of cooling load are obvious. Among them, factor $D$ ($SHGC$) is the main factor affecting the cooling load, followed by the $F$ ($ACH$), which is consistent with the findings of the literature [21] that window type and airtightness are the main factors affecting the energy saving of the envelope, lowering the heat gain from windows (reduce the heat transferred to the room through them) can improve the indoor thermal environment in summer. And the energy-saving goal can be achieved by

adding shading [74] or replacing high-performance external windows [21]. Furthermore, in order of importance, it is ranked as $D$ ($SHGC$) $> F$ ($ACH$) $> C$ ($\rho_s$) $> E$ ($K_{win}$) $> A$ ($W_{ins}$) $> B$ ($K_{wall}$) for SCZ and CZ, but the difference is $E > C$ in Lhasa, the main reason is that the higher solar radiation intensity in Lhasa and the larger window-to-wall ratio (WWR) of university teaching-office building makes the indoor heat affected by direct solar radiation much greater than the wall. This indicates that the differences in their microclimatic environments (solar radiation and outdoor temperature) make the focus of energy-saving strategies different even if they belong to the same climate zone. So it should not only combine the climate zones but also the local micro-climate when energy-saving strategies are proposed to maximize the benefits. Additionally, the rest are $D > F > E > C > A > B$ for the HSCW and HSWW
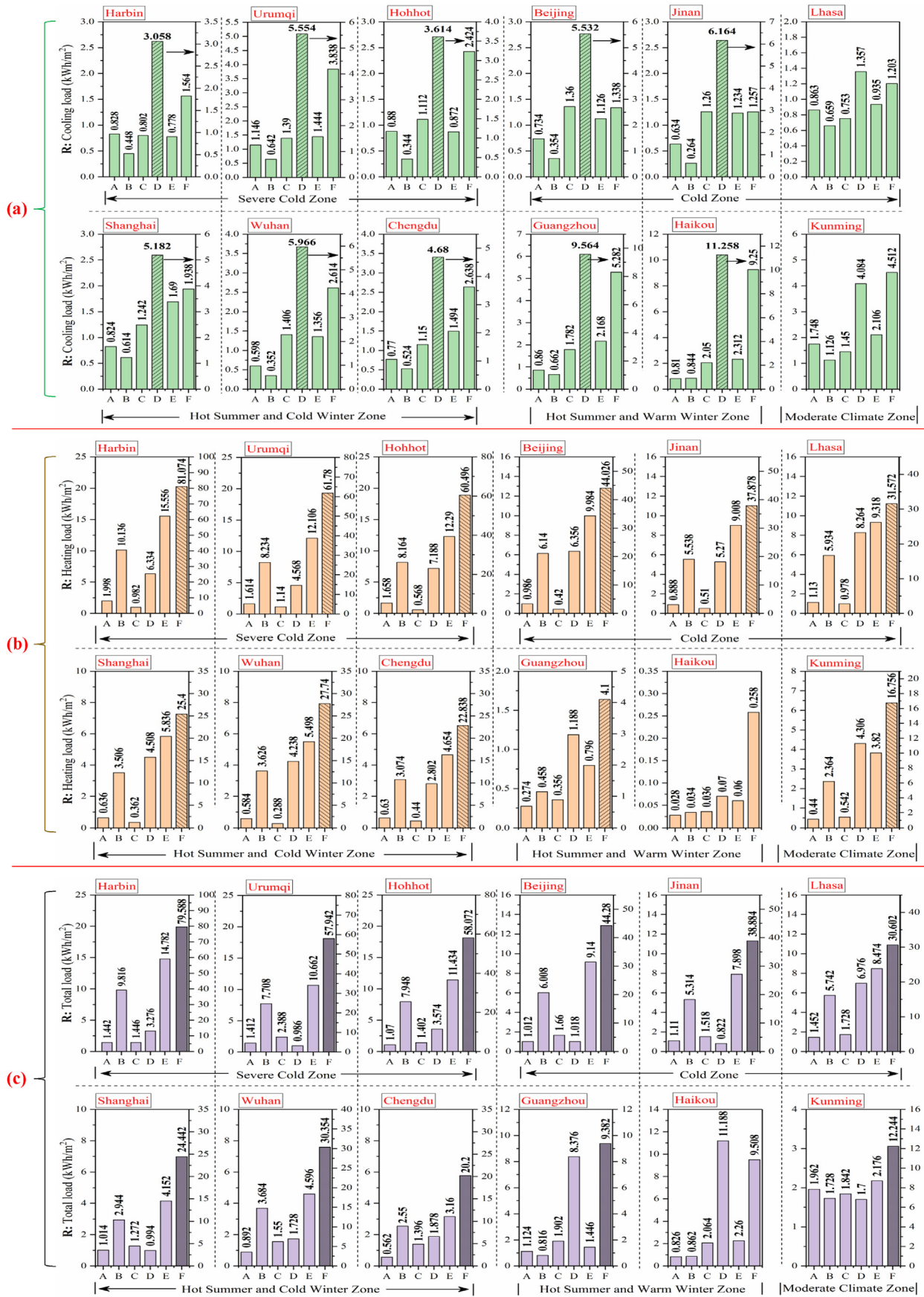
**Figure 10.** Influence degree of each factor of the envelope on the (a) cooling load, (b) heating load and (c) total load in different climates/cities.

except for Wuhan where $C > E$. It shows that for different regions the thermal performance of the walls is a much lower impact on the cooling load than external windows for university teaching-office buildings. However, the influence degree of each factor from the Kunming (MCZ) is ranked as $F > D > E > C > A > B$, the influence of $F$ on the cooling load is clearly higher than that of $D$, indicating that ventilation with an open window is the primary choice to improve the indoor thermal environment in the suitable climate zones. In general, $D$ and $F$ have the highest impact and $B$ is the lowest for cooling load in most zones for teaching-office buildings, which further suggests that the emphasis can be placed on improving the building's $K_{win}$, $SHGC$, and improving indoor ventilation to reduce the building's cooling load in higher WWR buildings.

In addition, for the heating load, there is often an opposite conclusion to the cooling load in the importance ordering of the influencing factors and the taken values. It can be observed from Figure 10 (b) that the factor $D$ which has a great influence on the cooling load is weakened on the heating load, while $F$ still shows a significant effect (ranking first). The variation is greater for factors $B$ and $C$, the effect of $B$ on the cooling load is smaller but on the heating cannot be ignored, while factor $C$ has essentially no effect on the heating load. It means that the emphasis on envelope energy-saving factors of concern is different in areas with different cooling and heating demands, such as the importance of insulation of walls is significantly higher in winter than in summer, and optimization of factor $B$ should focus on winter insulation rather than summer blocking the outdoor heat [14]. In addition, the importance ranking of each factor of the envelope for the SCZ and CZ (except Lhasa) on the heating load are $F > E > B > D > A > C$. While the Lhasa is consistent in other importance rankings, $D$ has a much greater impact on heating load than $B$, demonstrating that the heat gain through windows in high solar radiation areas is not negligible in either winter or summer. The importance ranking of the HSCW (except Chengdu) is $F > E > D > B > A > C$ on heating load, while the high humidity and low solar radiation in Chengdu cause the situation of $B > D$. Nevertheless, for Guangzhou, Haikou, and Kunming, where the temperature is relatively high, $D$ is the most important except for $F$, and their ranking is $F > D > E > B > C > A$. Meanwhile, it can be noticed from the above ranking that the importance of factor $D$ increases as the average temperature of the different thermal zones increases (from SCZ to HSWW), suggesting that areas with a lower heating load demand (or higher cooling load demand) should focus on the heat gained through external windows.

It is clear from the above analysis that different factors of the building envelope have different effects on the cooling and heating loads. However, the influence degree of each factor is discussed in this paper from the perspective of annual load considering that the thermal parameters of the building envelope do not change intermittently according to the seasons, and the results are shown in Figure 10(c). Factor $F$ still is the largest, which means that the energy saving of building loads can be remarkably improved by adjusting the $ACH$ appropriately in winter and summer. Then, factors $B$ and $E$ have a higher impact in the SCZ, CZ, and HSCW compared to others, while they have a lower impact in the warmer regions (Guangzhou and Haikou). It demonstrates that effective thermal insulation is a priority for year-round energy saving for northern heating areas in China. Nevertheless, factors $A$, $C$ and $D$ all have lower impact levels in most of China (except for Guangzhou, Haikou and Kunming), further concluding that the form of insulation (factor $A$) has a smaller impact on the annual total load and is much less important than the other factors, it is consistent with the finding in [8]. At the same time, it can be watched from the annual total load (factor $D$ is weakened) that although factor $D$ has a higher degree of influence on the cooling load for the northern thermal zones (SCZ, CZ) it is much less influential than on the heating load, however, it still differs in their impact levels for annual total load, which exhibits a higher influence on the HSWW. Among them, the important ordering of $A$, $C$, and $D$ mainly into $D > C > A$ (Hohhot, Lhasa, Wuhan, and Chengdu) and $C > A > D$ (Urumqi, Jinan, and Shanghai), and the influence degree of factors $F$, $E$ and $B$ on the total load is $F > E > B$

in the SCZ, CZ, and HSCW. However, there are also large differences in the ordering of the factors for the HSWW (Guangzhou and Haikou), with $F > D > C > E > A > B$ for Guangzhou and $F > D > E > C > B > A$ for Haikou. It shows that the priority of energy-saving factors is also different in areas with higher cooling demand (HSWW), which is mainly related to the local micro-climate environment. For Kunming (MCZ), the differences in importance are smaller except for $F$ but there is still a certain order ($F > E > A > C > B > E$). Based on the above results, the importance of energy-saving factors in the envelope varies from place to place, and it is particularly necessary to target important factors in the envelope for energy-saving retrofits considering the economic benefits [21, 75].

### 3.2.2. Suitability levels of each factor

Based on the above analysis, it is found that although each factor of the envelope has different influence degrees on the load, there exists a suitable value, which can be obtained intuitively by the orthogonal table (see Figure 9). However, whether there is a better level combination outside the 25 schemes needs to be determined by further calculations. For this reason, Figure 11 gives the influence laws of each factor ($m$) with different levels ($i$) on load based on the average target deviation ($K_{i,m}$) (the factors are expressed as $A$-$F$, and the levels of each factor are expressed as 1–5, and the detail values are shown in Table 5). Taking factor $A$ in Urumqi (SCZ) as an example, the cooling load is shown in Figure 11(a), corresponding to level 1–5 are 5.6 kWh/m$^2$, 6.7 kWh/m$^2$, 5.9 kWh/m$^2$, 6.1 kWh/m$^2$ and 6.0 kWh/m$^2$,respectively. That is to say, factor A achieves the lowest building energy consumption at Level 1. In the same way, factors $B$, $C$, $D$, $E$, and $F$ achieve the lowest building energy consumption at Level 1, Level 5, Level 1, Level 1, Level 5, and Level 5, respectively. When the optimal level of each factor is combined, a new optimal combination represented by $A_1B_5C_1D_1E_5F_5$ is generated. Similarly, the optimal combination of cooling loads for the other cities in the SCZ can be derived as $A_1B_5C_1D_1E_3F_5$ (Hohhot) and $A_1B_5C_1D_1E_2F_3$ (Harbin). The combination of the above clearly reveals that there are remarkable regional differences in the optimization of each factor even if they belong to the same thermal zone, for example, factor $E$ ($K_{wall}$), where the requirement for wall insulation performance is higher in Harbin than in the other two cities. Furthermore, for the most important factor $D$ affecting the cooling load, the optimal value for the SHGC in Urumqi is taken as $D_1$ (0.35), and the cooling load is increased by 147% as the level is raised from $D_1$ to $D_5$ (from 0.35 to 0.75). While for factor B with low influence, the increase in level from $B_1$ [0.2 W/(m$^2$·K)] to $B_5$ [1.0 W/(m$^2$·K)] only reduces the cooling load by 9%. The above data further illustrates the importance of optimizing the important factors of the envelope. Then from other factors, the changing trend of cooling load under the level change is basically the same, the biggest difference is factor $F$, the lower the $F$ in the SCZ, the higher the cooling load, suggesting that more open-window ventilation should be carried out in the SCZ (summer), but the ventilation should be minimized in areas with high average summer temperatures (Guangzhou and Haikou). However, $F$-optimal levels show large differences even in the same climatic zone. For the example of HSCW, the optimal level of factor $F$ is $F_3$ (1.5/hr) in Shanghai, $F_1$ (0.5/hr) in Wuhan, and $F_5$ (2.5/hr) in Chengdu. In addition, the load corresponding to the same factor at the optimum level varies considerably whether in the same climatic region or different, such as factor $A$, the cooling load (compared to the lowest value) differs by 30%–72% (SCZ), 28%–1309% (CZ), 33%–133% (HSCW) and 36% (HSWW) for the same climate zone. So it can be suggested that the different load requirements should be referenced when optimizing the energy-saving factors of the envelope.

Moreover, on a single factor, the exterior insulation walls ($E_w$) is more suitable for energy-saving of cooling load in most areas (see Figure 11(a)), the interior insulation wall ($I_w$) shows optimal energy savings on heating loads in SCZ, CZ and HSCW (except Shanghai and Lhasa) (see Figure 11(b)). The main reason is that the lower thermal conductivity of the second layer of material in the wall impedes the heat transfer from indoors to the outdoors for the high heating demand in
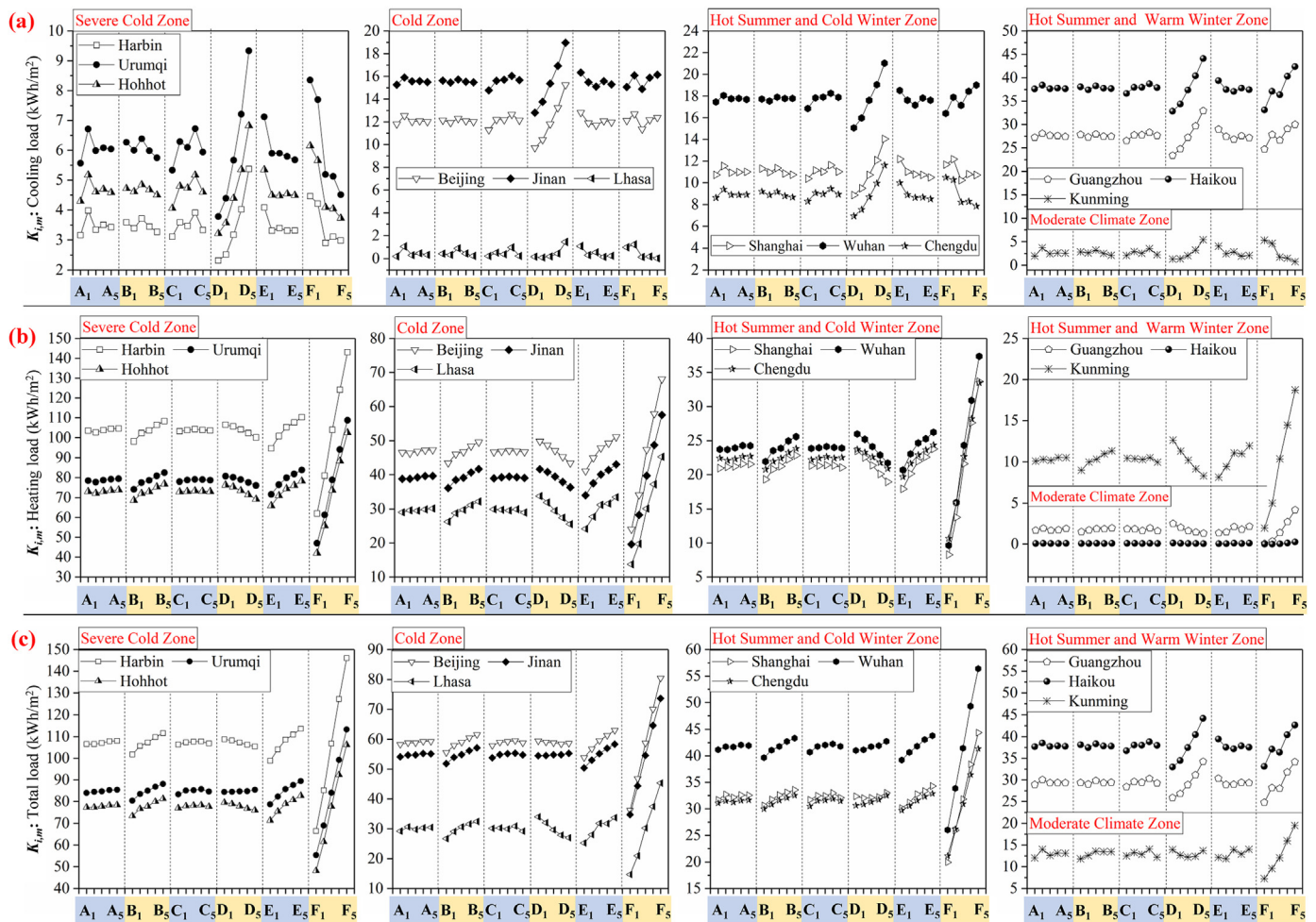
**Figure 11.** Effect of the level of each factor of the envelope on (a) cooling load, (b) heating load and (c) total load in different climates/cities.

winter [38], so there is also a phenomenon of energy-saving in winter and energy-consumption in summer, especially in areas with high cooling and heating demand is more evident. While, although there are some differences between different cities for the wall with different heat storage coefficients ($L_w$ and $H_w$), its advantages can be ignored compared with the insulation layer location. As for factor $B$, it's lower the more energy-saving for cities with high heating demand, while it is obvious for cities with high cooling demand that the higher energy consumption [76]. Which makes further explains that the lower $B$ ($K_{wall}$) can effectively block the heat transfer from indoor to outdoor, and increase the cooling load despite the reduced heating load. Meanwhile, it can be seen from Figure 11(a) and (b) that the lower the factor $C$ ($\rho_s$), the lower the cooling load, while the heating load remains essentially unchanged. It is mainly caused by the phenomenon the lower $C$ can reflect most of the high direct radiation and scattered radiation heat from the outside through the outer surface of the wall in summer to prevent outdoor heat from being transferred to the indoor by the heat conduction of the external wall [18], but its optimization is less meaningful in winter due to lower solar radiation and higher window-wall ratio. Whereas $E$ ($K_{win}$) does not lower the more energy-saving in summer, different regions have different optimal values which are chosen as 2.5 W/(m²·K) (Harbin), 4.5 W/(m²·K) (Lhasa, Kunming), 5.5 W/(m²·K) (Urumqi, Shanghai, and Chengdu) and 3.5 W/(m²·K) (other cities), respectively. However, as the levels of factors $B$ and $E$ are increased from $B_1$ ($E_1$) to $B_5$ ($E_5$) in winter (see Figure 11(b)), the heating load is significantly raised, which is taken as $B_1$ [0.2 W/(m²·K)] and $E_1$ [1.5 W/(m²·K)] is the most energy-saving for all cities. Additionally, high $D$ can considerably reduce the heating

load, and taken as 0.75 is more suitable in most areas of China but has a high negative impact on the cooling load. As a result, window shading is a more effective measure to balance winter and summer energy requirements [43]. Finally, factor $F$ is the key to energy saving for all regions in winter and should be minimized to reduce cold air infiltration, as can be seen from Figure 11(b), factor $F$ reduces by $F_1$ (0.5/hr) from $F_5$ (2.5/hr), the heating load in each region is cut by 57%–59% (SCZ), 65%–70% (CZ), 68%–75% (HSCW), 98%–100% (HSWW) and 90% (MCZ).

Besides, given that the level of the envelope factors is less likely to change during the whole year, the appropriate levels of all factors for the year-round operating conditions are given in Figure 11(c), which yields that $F$ is still the lower the more energy-saving. Also, $A_1$ ($E_w$) performs better in the annual load although $A_2$ ($I_w$) helps to reduce the heating load. The lower the $B$ [set to 0.2 W/(m²·K)] is more energy-saving for most cities except for the HSWW which should be set to 0.4 W/(m²·K). Factor $C$ is lower and more energy-saving (set to 0.15) in all cities except for Kunming and Lhasa where higher values are better (set to 0.75). However, the optimal level of $D$ varies in different cities in the same climate zone, take the CZ as an example, Jinan and Lhasa are taken as the lowest 0.35 and the highest 0.75, separately. 0.75 is taken for SCZ (Urumqi is 0.35). The lower the value of $D$ in HSCW and HSWW, the more energy-saving it is (set to 0.35), and the MCZ is set to 0.55. The reason for the above large disparities is that different cities have different proportions of cooling and heating load, and when the cooling load is higher (or lower) than the heating load, the annual optimal value is biased towards the side with higher demand. For factor $E$, all cities except for Kunming, Guangzhou, and Haikou exhibit lower $K_{win}$ [set to 1.5 W/
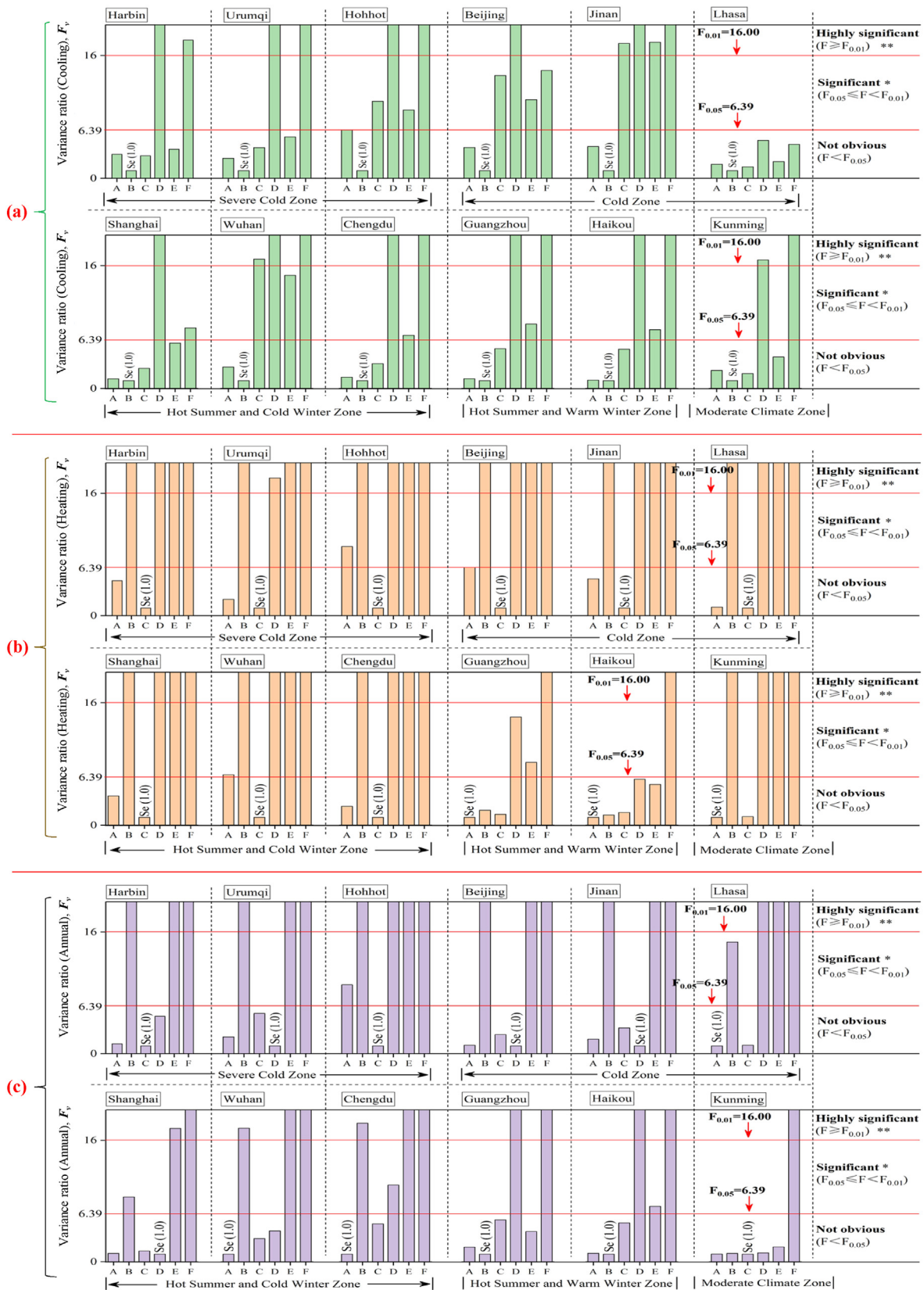
**Figure 12.** Variance and significance level of each factor of the envelope in (a) cooling load, (b) heating load and (c) total load for different climates/cities.

$(m^2 \cdot K)]$ more energy saving. It can be concluded from the above data that the suitable level and the influence degree (energy saving sensitivity) of each factor of the envelope are widely divergent from region to region,

and it is necessary to provide the optimal solution for the different factors of envelopes in different regions to achieve maximum energy-saving building operations.

14

**Table 10.** Optimal combination scheme and order of influencing factors for 12 cities in summer/winter and the whole year.

| Climate zone | City | Summer | | CL (kWh/m²) | Winter | | HL (kWh/m²) | Whole year | | TL (kWh/m²) |
|---|---|---|---|---|---|---|---|---|---|---|
| | | Optimal combination[1] | Factor Impact Degree | | Optimal combination[1] | Factor Impact Degree | | Optimal combination[1] | Factor Impact Degree | |
| SCZ | HRB | $A_1B_5C_1D_1E_2F_3$ | D**>F**>A > C > E > B | 1.4 (75.82%) | $A_2B_1C_1D_5E_1F_1$ | F**>E**>B**>D**>A>C | 39.99 (60.7%) | $A_2B_1C_1D_5E_1F_1$ | F**>E**>B**>D>C>A | 50.59 (52.97%) |
| | URQ | $A_1B_5C_1D_1E_5F_5$ | D**>F**>E>C>A>B | 2.38 (75.0%) | $A_2B_1C_1D_5E_1F_1$ | F**>E**>B**>D**>A>C | 29.80 (60.6%) | $A_1B_1C_1D_1E_1F_1$ | F**>E**>B**>C>A>D | 42.85 (49.68%) |
| | HOT | $A_1B_5C_1D_1E_3F_5$ | D**>F**>C*>A > E*>B | 1.92 (78.18%) | $A_2B_1C_1D_5E_1F_1$ | F**>E**>B**>D**>A*>C | 23.19 (66.58%) | $A_1B_1C_1D_5E_1F_1$ | F**>E**>B**>D>C>A* | 35.36 (54.78%) |
| CZ | BJ | $A_1B_2C_1D_1E_3F_3$ | D**>C*>F*>E*>A > B | 8.03 (49.97%) | $A_2B_1C_1D_5E_1F_1$ | F**>E**>D**>B**>A>C | 10.62 (74.38%) | $A_1B_1C_1D_4E_1F_1$ | F**>E**>B**>C > D > A | 27.57 (52.06%) |
| | JN | $A_1B_2C_1D_1E_3F_3$ | D**>F**>C**>E**>A > B | 11.06 (50.14%) | $A_1B_1C_1D_5E_1F_1$ | F**>E**>B**>D**>A>C | 7.90 (76.5%) | $A_1B_1C_1D_1E_1F_1$ | F**>E**>B**>C>A>D | 25.73 (53.88%) |
| | LS | $A_1B_5C_1D_2E_4F_5$ | D > F > E>A>C>B | 0 (100%) | $A_1B_1C_5D_5E_1F_1$ | F**>E**>D**>B**>A>C | 3.01 (86.47%) | $A_1B_1C_5D_5E_1F_1$ | F**>E**>D**>B*>C>A | 14.62 (39.64%) |
| HSCW | SH | $A_1B_5C_1D_1E_5F_3$ | D**>F**>E>C>A>B | 7.38 (60.26%) | $A_1B_1C_5D_5E_1F_1$ | F**>E**>D**>B**>A>C | 2.08 (86.48%) | $A_1B_1C_1D_2E_1F_1$ | F**>E**>B**>C>A>D | 15.39 (54.68%) |
| | WH | $A_1B_2C_1D_1E_3F_1$ | D**>F**>C**>E*>A > B | 11.51 (52.26%) | $A_2B_1C_1D_5E_1F_1$ | F**>E**>D**>B**>A*>C | 2.54 (85.85%) | $A_1B_1C_1D_1E_1F_1$ | F**>E**>B**>D>C>A | 19.39 (53.9%) |
| | CD | $A_1B_5C_1D_1E_5F_5$ | D**>F**>E*>C>A>B | 5.61 (66.16%) | $A_2B_1C_1D_5E_1F_1$ | F**>E**>B**>D**>A>C | 4.32 (73.66%) | $A_1B_1C_1D_1E_1F_1$ | F**>E**>B**>D>C>A | 16.09 (51.21%) |
| MCZ | KM | $A_1B_5C_1D_1E_4F_5$ | F**>D**>E>A>C>B | 0.17 (98.19%) | $A_1B_1C_5D_5E_1F_1$ | F**>D**>E**>B**>C>A | 0.03 (99.33%) | $A_1B_1C_5D_3E_2F_1$ | F**>E>A>C>B > D | 6.71 (51.52%) |
| HSWW | GZ | $A_1B_2C_1D_1E_3F_1$ | D**>F**>E*>C>A>B | 17.56 (58.87%) | $A_1B_2C_5D_5E_1F_1$ | F**>D*>E*>B>C>A | 0 (100%) | $A_1B_2C_1D_1E_2F_1$ | F**>D**>C > E > A > B | 18.26 (51.21%) |
| | HK | $A_1B_2C_1D_1E_3F_1$ | D**>F**>E*>C > B > A | 24.11 (57.61%) | $A_4B_1C_3D_5E_1F_1$ | F**>D > E > C > B > A | 0 (100%) | $A_1B_2C_1D_1E_3F_1$ | F**>D**>E*>C > B > A | 24.11 (57.57%) |

Note: "** " = Highly significant; "* " = Significant; "Unmarked " = Not obvious; 1 = Each combination of parameters in Table 5; CL = Cooling Load, kWh/m²; HL = Heating Load, kWh/m²; TL = Total Load, kWh/m².

### 3.3. Significance of influencing factors

The importance ordering and optimal level of each factor are obtained by the above results, but it is especially necessary to optimize the salience influencing factors considering the practical engineering problems. Therefore, the analysis of variance (ANOVA) is used in this paper to determine the significance level of each factor. Considering the large differences of each factor among cities, the minimum value of the sum of the squared deviation of each factor in different cities is used as the error analysis condition, denoted by $S_e$. If the variance ratio ($F_v$) of some factor is higher than the $F_{0.01}$ (16.00), it means that this factor has a significant influence on the building load with a 99% possibility. If $F_{0.05}$ (6.39) $\leq F_v$ < $F_{0.01}$ (16.00), the possibility then drops to 95%. At the same time, if $F_v$ < $F_{0.05}$ indicates that the factor has no statistically significant effect on the study objectives.

Figure 12 presents the significance levels of each factor on cooling, heating, and total load in different climates, it can be obtained from Figure 12(a) that for the SCZ, factors *D* and *F* have a high significance on cooling load ($F_v \geq F_{0.01}$), while *C* and *E* only show a significant on Hohhot, other factors are not obvious. The results show that the main factors are very different even in the same climate zone due to geographical differences, and this phenomenon is more obvious in the CZ. *C*, *D*, *E,* and *F* all show the significance for Beijing and Jinan, but none of the factors for the Lhasa. Furthermore, factor *B* which can be ignored in the cooling load is the most prominent in the heating load (except for Guangzhou and Haikou). Among all factors, *B*, *D*, *E,* and *F* show high significance in most areas of China for the heating load as in Figure 12(b). It implies a necessity to use some energy-saving techniques to improve the insulation, heat gain, and airtightness of the envelope in winter for more effective energy savings, for example, adding insulation materials [14, 77], Trombe-wall [9, 10, 11, 49], solar air collectors [78], low-E windows [79] and improving the airtightness of exterior windows [80]. However, *A* shows a certain significance only in Hohhot. This indicates that the form of insulation is far less important to study than other factors for most regions in China. As well, it is evident in HSWW that only factors *D, E,* and *F* in Guangzhou and *F* in Haikou are significant influencing factors in terms of the highly significant factors in heating load (*B*, *D*, *E*, and *F*), which further suggests that teaching-office buildings only need to improve the thermal performance of windows in regions with low or no heating demand. The factor *C* has essentially no effect on the heating load. It is mainly because the higher WWR makes the solar heat gain through the non-transparent envelope is basically negligible for the heat loss of the whole building, which is sufficient to explain the difference between university buildings and other buildings in energy-saving strategies.

Considering the fixed thermal parameters of the envelope, it is more helpful to optimize the overall performance of the building envelope by identifying the main influencing factors from the perspective of the annual total load. As shown in Figure 12(c), the highly significant factors of total load are *B*, *E,* and *F* (except Guangzhou, Haikou, and Kunming), of these, the Kunming only needs to focus on factor *F*, and the high significance of factor *D* is only exhibited in Hohhot, Lhasa, Guangzhou, and Haikou. The results point out that we have to prioritize the insulation and ventilation of the exterior windows in our energy-saving strategies from the annual load perspective. Meanwhile, *D* is very significant in Hohhot but its effect is largely negligible in Harbin and Urumqi, and the above phenomenon (there are differences in the main factors under the same climate) is also more obvious in the CZ. As a result, the main energy-saving factors of the envelope differ even in the same climate zone, further explaining that the thermal performance of the envelope of teaching-office buildings in different climate zones and cities should be optimized on the basis of climate zoning in combination with local microclimate and load demands.

### 3.4. Optimization results under different climates/cities

Combining the above analysis for cooling and heating load of typical cities in different climates, Table 10 gives the optimal combination scheme, significance, and important order of each factor under different climatic conditions. It can be concluded that when only winter or summer conditions are considered, optimized envelope factors based on cooling or heating demand result in energy savings of 49.97%–100% for cooling load and 60.6%–100% for heating load between different climates/cities. That is to say, optimizing the exterior envelope can make the season reach nearly zero energy consumption (NZE) in some cities with low heating or cooling demand. In addition, the average energy saving rates for different climate zones can be seen from the cooling/heating load alone are 98.19%/99.33% (MCZ), 76.33%/63.62% (SCZ), 66.7%/79.12% (CZ), 59.56%/81.99% (HSCW) and 58.24%/100% (HSWW), respectively, and it begins to be weakened as the cooling/heating load demand is enhanced, but it is still above 59.56%. The above results show that the higher cooling/heating load can be significantly reduced by optimizing the building envelope but do not achieve ZNE. While more energy-saving factors need to be considered to achieve the goal of carbon neutrality, such as air conditioning setting temperature, air conditioning running time, personnel density, and other indoor and outdoor thermal disturbances, as well as the application of passive energy-saving technologies, such as shading systems [81], double-cooling/heating systems [82], and solar energy utilization systems [83]. Moreover, considering that the thermal properties of the envelope will not be intermittently replaced due to seasonal differences, energy-saving design from a whole year perspective is more in line with the operational characteristics of the building. Therefore, Table 10 gives the optimized solutions for whole year operating conditions. It can be found that the annual load energy saving rates can reach 39.64%–57.57% in different climate zones/cities, while the energy-saving rates are noticeably lower compared to considering only cooling or heating loads. For example, for SCZ, the average energy-saving rates for cooling and heating load are 76.33% and 63.62%, respectively, whereas the energy-saving rate is reduced to 52.48% when optimizing from a year-round perspective. The above phenomenon is caused by the fact that when considering energy savings for cooling load only, the negative impact on heating (it will be increased) is not considered in the optimization, and vice versa. As a result, when the designer gives different weighting coefficients to the envelope factors with different usage requirements (cooling and heating), different optimization options and energy-saving targets can be derived. However, it is more relevant to design for energy-saving from a whole year perspective when both cooling and heating demands for local buildings need to be considered.

## 4. Conclusions

The influence and adaptability of different thermal properties of university teaching-office building envelopes on energy consumption in 12 typical cities of China (different climates) are discussed in this paper through numerical simulations and orthogonal design. The importance ranking, influence degree, and optimal level of each factor (*A*-$W_{ins}$, *B*-$K_{wall}$, *C*-$\rho_s$, *D*-SHGC, *E*-$K_{win}$, *F*-ACH) on the cooling, heating, and annual total load under different climates/cities are obtained. The main conclusions are gained as follows:

- The cooling and heating load demands and optimization objectives vary considerably depending on the climatic conditions under the same thermal performance of the envelope. The heating load in the SCZ accounts for 88.75%–94.6% of the total load, which should focus on winter for energy-saving optimization. However, this share is reduced with the decrease of heating load demand in different cities

(cooling load is increased), and the heating load share approaches zero (the cooling load approaching 100%) in HSWW.

- The influence degree of each factor of the envelope on the load varies greatly in different climates. Among them, factors $D$ and $F$ ($E$ and $F$) are the main factors affecting the cooling (heating) load, and factors $A$ and $B$ ($A$ and $C$) have less influence. Among them, the impact of factor $B$ on the heating/annual load (SCZ, CZ, and HSCW) cannot be ignored even though its effect on the cooling load is minor.
- Among all cities, the important ranking of the influence of each factor on the cooling and heating loads is related to their load demands. For regions with high cooling load demands (HSCW and HSWW) the ranking are mainly $D > F > E > C > A > B$, While the ranking are $F > E > D > B > A > C$ for high heating load demands (SCZ and CZ). Conversely, in regions with low cooling or heating load requirements, the ranking varies geographically (even if they belong to the same thermal zone).
- Although each factor has a certain order of influence, the optimal level and saliency of these influence factors are different. Of these, the optimal level of each factor is somewhat negatively correlated with the local cooling (or heating) load demand. Moreover, factors $D$ and $F$ show high significance in all cities for cooling loads, while for heating loads the highly significant influences are $B$, $D$, $E$ and $F$. Based on the annual load, $B$ and $E$ are the priorities factor for energy savings in the northern heating regions of China while it is not obvious in Guangzhou, Haikou, and Kunming. Factors $A$, $C$, and $D$ are not obvious in most regions, among them, the high significance of $D$ is only shown in Hohhot, Lhasa, Guangzhou, and Haikou.
- External ($E_w$) and internal insulation ($I_w$) are suitable for cooling and heating load energy-saving, respectively, while the $E_w$ is the preferred choice based on annual load.
- The energy savings of optimized envelope factors is 49.97%–100% for cooling load and 60.6%–100% for heating load when only winter or summer conditions are considered. However, annual load energy savings can reach 39.64%–57.57% in different climatic zones when optimized based on annual operating conditions.

The cities selected for the study in this paper represent the climatic characteristics of different regions in China, and the proposed exterior envelope factors accurately indicate the thermal insulation and airtightness of the building. In the numerical study, the influence of each factor of the envelope of the university teaching-office building on cooling/heating load in different climates was analyzed and the optimization solutions of different cooling and heating demand were proposed. The research results can provide directions and data references for the energy-saving design and renovation of educational building envelopes in different climates (China).

## Declarations

### Author contribution statement

Zu'an Liu: Conceived and designed the experiments; Performed the experiments; Analyzed and interpreted the data; Contributed reagents, materials, analysis tools or data; Wrote the paper.

Jiawen Hou: Conceived and designed the experiment; Analyzed and interpreted the data; Contributed reagents, materials, analysis tools or data; Wrote the paper.

Lili Zhang: Conceived and designed the experiments; Contributed materials, Analysis tools and data.

Bart Julien Dewancker; Xi Meng: Analyzed and interpreted the data.

Chaoping Hou: Contributed reagents, materials, analysis tools or data.

## References

[1] China association building energy efficiency, China building energy consumption annual report 2019, Construction and Architecture 7 (2020) 30–39.

[2] E. Long, Z. Zang, X. Ma, Are the energy conservation rates (RVRs) approximate in different cities for the same building with the same outer-wall thermal insulation measures? Build. Environ. 40 (4) (2005) 537–544.

[3] W. Shen, Application Research of the Technology of green Building and green Building Materials about Colleges and Universities' Buildings-Taking Zhejiang College of Construction Training center Project as an Example, Master's thesis, Xi'an University of Architecture and Technology, Xi'an, Shanxi, China, 2013.

[4] K. Guo, L. Zhang, T. Wang, Optimal scheme in energy performance contracting under uncertainty: a real option perspective, J. Clean. Prod. 231 (2019) 240–253.

[5] X. Li, C. Shen, C.W.F. Yu, Building energy efficiency: passive technology or active technology? Indoor Built Environ. 26 (6) (2017) 729–732.

[6] L. Zhang, Y. Li, R. Stephenson, B. Ashuri, Valuation of energy efficient certificates in buildings, Energy Build. 158 (2018) 1226–1240.

[7] F. Harkouss, F. Fardoun, P.H. Biwole, Passive design optimization of low energy buildings in different climates, Energy 165 (2018) 591–613.

[8] J. Hou, T. Zhang, Z. Liu, L. Zhang, H. Fukuda, Application evaluation of passive energy-saving strategies in exterior envelopes for rural traditional dwellings in northeast of Sichuan hills, China, Int. J. Low Carbon Technol. 17 (2022) 342–355.

[9] K. Sergei, C. Shen, Y. Jiang, A review of the current work potential of a trombe wall, Renew. Sustain. Energy Rev. 130 (2020), 109947.

[10] M. Dhahri, N. Khalilpoor, H. Aouinet, A. Issakhov, H. Sammouda, S. Emani, Numerical study on the thermal performance of trombe wall for passive solar building in semiarid climate, Int. J. Photoenergy 2021 (2021) 1–12.

[11] Y. Zhu, T. Zhang, Q. Ma, H. Fukuda, Thermal performance and optimizing of composite trombe wall with temperature-controlled DC fan in winter, Sustainability 14 (5) (2022) 3080.

[12] F. Roberz, R. Loonen, P. Hoes, J.L.M. Hensen, Ultra-lightweight concrete: energy and comfort performance evaluation in relation to buildings with low and high thermal mass, Energy Build. 138 (2017) 432–442.

[13] J. Shi, B. Liu, Z. He, Y. Liu, J. Jiang, T. Xiong, J. Shi, A green ultra-lightweight chemically foamed concrete for building exterior: a feasibility study, J. Clean. Prod. 288 (2021), 125085.

[14] L. Zhang, Z. Liu, C. Hou, J. Hou, D. Wei, Y. Hou, Optimization analysis of thermal insulation layer attributes of building envelope exterior wall based on DeST and life cycle economic evaluation, Case Stud. Therm. Eng. 14 (2019), 100410.

[15] Z. Liu, J. Hou, Y. Huang, J. Zhang, X. Meng, B.J. Dewancker, Influence of phase change material (PCM) parameters on the thermal performance of lightweight building walls with different thermal resistances, Case Stud. Therm. Eng. 31 (2022), 101844.

[16] Y. Li, E. Long, P. Ding, S. Guo, Characteristics optimization of composite phase-change wall during intermittent heating process, Sci Technol Built Environ 26 (4) (2020) 541–551.

[17] Y. Li, E. Long, Z. Jin, J. Li, X. Meng, J. Zhou, L. Xu, D. Xiao, Heat storage and release characteristics of composite phase change wall under different intermittent heating conditions, Sci Technol Built Environ 25 (3) (2019) 336–345.

[18] J. Wang, S. Liu, X. Meng, W. Gao, J. Yuan, Application of retro-reflective materials in urban buildings: a comprehensive review, Energy Build. 247 (2021), 111137.

[19] W. Hong, R. Guo, H. Tang, Potential assessment and implementation strategy for roof greening in highly urbanized areas: a case study in Shenzhen, China, Cities 95 (2019), 102468.

[20] J. Dong, M. Lin, J. Zuo, T. Lin, J. Liu, C. Sun, J. Luo, Quantitative study on the cooling effect of green roofs in a high-density urban Area—a case study of Xiamen, China, J. Clean. Prod. 255 (2020), 120152.

[21] H.X. Li, Y. Li, B. Jiang, L. Zhang, X. Wu, J. Lin, Energy performance optimisation of building envelope retrofit through integrated orthogonal arrays with data envelopment analysis, Renew. Energy 149 (2020) 1414–1423.

[22] T.M. Echenagucia, A. Capozzoli, Y. Cascone, M. Sassone, The early design stage of a building envelope: multi-objective search through heating, cooling and lighting energy performance analysis, Appl. Energy 154 (2015) 577–591.

[23] L.D.O. Neves, T.H.T. Marque, Building envelope energy performance of high-rise office buildings in Sao Paulo city, Brazil, Procedia Environ. Sci. 38 (2017) 821–829.

[24] C.A. Balaras, K. Droutsa, A.A. Argiriou, D.N. Asimakopoulos, Potential for energy conservation in apartment buildings, Energy Build. 31 (2) (2000) 143–154.

[25] G. Semprini, C. Marinosci, A. Ferrante, G. Predari, G. Mochi, M. Garai, R. Gulli, Energy management in public institutional and educational buildings: the case of the school of engineering and architecture in Bologna, Energy Build. 126 (2016) 365–374.

[26] A. Charles, W. Maref, C.M. Ouellet-Plamondon, Case study of the upgrade of an existing office building for low energy consumption and low carbon emissions, Energy Build. 183 (2019) 151–160.

[27] M. Braulio-Gonzalo, M.D. Bovea, Environmental and cost performance of building's envelope insulation materials to reduce energy demand: thickness optimization, Energy Build. 150 (2017) 527–545.

[28] J. Hou, T. Zhang, Z. Liu, C. Hou, H. Fukuda, A study on influencing factors of optimum insulation thickness of exterior walls for rural traditional dwellings in northeast of Sichuan hills, China, Case Stud. Constr. Mater. 16 (2022), e01033.

[29] Y. Yu, L. Cai, Y. Wang, J. Wang, X. Zhang, Energy-saving transformation research on the external wall of existing residential buildings in nanjing area, Proceedings of ECOS 2013-the 26th I International Conference on Efficiency, Cost, Optimization, Simulation and Environmental Impact of Energy Systems (2013) 1–6.

[30] F. Leccese, G. Salvadori, F. Asdrubali, P. Gori, Passive thermal behaviour of buildings: performance of external multi-layered walls and influence of internal walls, Appl. Energy 225 (2018) 1078–1089.

[31] H.X. Li, L. Zhang, D. Mah, H. Yu, An integrated simulation and optimization approach for reducing CO2 emissions from on-site construction process in cold regions, Energy Build. 138 (2017) 666–675.

[32] F. Ascione, N. Bianco, G.M. Mauro, D.F. Napolitano, Building envelope design: multi-objective optimization to minimize energy consumption, global cost and thermal discomfort. Application to different Italian climatic zones, Energy 174 (2019) 359–374.

[33] E. Mostavi, S. Asadi, D. Boussaa, Framework for energy-efficient building envelope design optimization tool, J. Architect. Eng. 24 (2) (2018), 04018008.

[34] Y. Huang, J. Niu, Optimal building envelope design based on simulated performance: history, current status and new potentials, Energy Build. 117 (2016) 387–398.

[35] I.G. Capeluto, C.E. Ochoa, Simulation-based method to determine climatic energy strategies of an adaptable building retrofit façade system, Energy 76 (2014) 375–384.

[36] L. Zhang, T. Luo, X. Meng, Y. Wang, C. Hou, E. Long, Effect of the thermal insulation layer location on wall dynamic thermal response rate under the air-conditioning intermittent operation, Case Stud. Therm. Eng. 10 (2017) 79–85.

[37] X. Meng, Y. Huang, Y. Cao, Y. Gao, C. Hou, L. Zhang, Q. Shen, Optimization of the wall thermal insulation characteristics based on the intermittent heating operation, Case Stud. Constr. Mater. 9 (2018), e00188.

[38] X. Meng, T. Luo, Y. Gao, L. Zhang, X. Huang, Comparative analysis on thermal performance of different wall insulation forms under the air-conditioning intermittent operation in summer, Appl. Therm. Eng. 130 (2018) 429–438.

[39] P. Xu, X. Zhai, Influence of climate and building envelope on performance of air source heat pump air conditioning system, CIE J. 67 (2) (2016) 208–216.

[40] M. Košir, L. Pajek, N. Iglič, R. Kunič, A theoretical study on a coupled effect of building envelope solar properties and thermal transmittance on the thermal response of an office cell, Sol. Energy 174 (2018) 669–682.

[41] X. Zhou, D. Yan, J. An, T. Hong, X. Shi, X. Jin, Comparative study of air-conditioning energy use of four office buildings in China and USA, Energy Build. 169 (2018) 344–352.

[42] L. Qi, The Study of Heat Transfer and Energy Saving of School Building—Taking a University Library in Hangzhou as Example, Master's Thesis, Zhejiang Sci-Tech University, Hangzhou, Zhejiang, China, 2018.

[43] L. Pan, Q. Xu, Y. Nie, T. Qiu, Analysis of climate adaptive energy-saving technology approaches to residential building envelope in Shanghai, J. Build. Eng. 19 (2018) 266–272.

[44] Y. Lyu, W. Liu, H. Su, X. Wu, Numerical analysis on the advantages of evacuated gap insulation of vacuum-water flow window in building energy saving under various climates, Energy 175 (2019) 353–364.

[45] M. Aburas, V. Soebarto, T. Williamson, R. Liang, H. Ebendorff-Heidepriem, Y. Wu, Thermochromic smart window technologies for building application: a review, Appl. Energy 255 (2019), 113522.

[46] W. Sun, H. Jin, A Study on Energy Saving Design Strategies of Universities' Education Building in the Cold Zone of China, 5th International Conference on Responsive Manufacturing-Green Manufacturing, ICRM 2010) IET, 2010, pp. 100–105.

[47] H. Ma, N. Du, S. Yu, W. Lu, Z. Zhang, N. Deng, C. Li, Analysis of typical public building energy consumption in northern China, Energy Build. 136 (2017) 139–150.

[48] H. Huo, J. Shao, H. Huo, Contributions of energy-saving technologies to building energy saving in different climatic regions of China, Appl. Therm. Eng. 124 (2017) 1159–1168.

[49] L. Zhang, Y. Hou, Z. Liu, J. Du, L. Xu, G. Zhang, L. Shi, Trombe wall for a residential building in Sichuan-Tibet alpine valley–A case study, Renew. Energy 156 (2020) 31–46.

[50] W. Zuo, E. Jiaqiang, X. Liu, Q. Peng, Y. Deng, H. Zhu, Orthogonal experimental design and fuzzy grey relational analysis for emitter efficiency of the micro-cylindrical combustor with a step, Appl. Therm. Eng. 103 (2016) 945–951.

[51] E. Jiaqiang, D. Han, A. Qiu, H. Zhu, Y. Deng, J. Chen, X. Zhao, W. Zuo, H. Wang, J. Chen, Q. Peng, Orthogonal experimental design of liquid-cooling structure on the cooling effect of a liquid-cooled battery thermal management system, Appl. Therm. Eng. 132 (2018) 508–520.

[52] Y. Xiong, Y. Pan, L. Wu, B. Liu, Effective weight-reduction-and crashworthiness-analysis of a vehicle's battery-pack system via orthogonal experimental design and response surface methodology, Eng. Fail. Anal. 128 (2021), 105635.

[53] L. Fang, X. Liao, Q. Zhang, L. Shi, L. Zhou, H. Zhao, W. Kong, An orthogonal experimental design and QuEChERS based UFLC-MS/MS for multi-pesticides and human exposure risk assessment in Honeysuckle, Ind. Crop. Prod. 164 (2021), 113384.

[54] Y. Sun, C. Li, J. You, C. Bu, L. Yu, Z. Yan, X. Liu, Y. Zhang, X. Chen, An investigation of the properties of expanded polystyrene concrete with fibers based on an orthogonal experimental design, Materials 15 (3) (2022) 1228.

[55] B. Liu, L. Sha, K. Huang, W. Zhang, A topology optimization method for collaborative robot lightweight design based on orthogonal experiment and its applications, Int. J. Adv. Rob. Syst. 19 (1) (2022), 17298814211056143.

[56] Ministry of housing, urban-rural development, Code for Thermal Design of Civil Building (GB 50176-2016), China Architecture & Building Press, Beijing, China, 2016.

[57] D. Wei, L. Yang, Z. Bao, Y. Lu, H. Yang, Variations in outdoor thermal comfort in an urban park in the hot-summer and cold-winter region of China, Sustainable Cities and Society 77 (2022), 103535.

[58] EnergyPlus. https://energyplus.net/weather-region/asia_wmo_region_2/CHN, 2021. (Accessed 4 October 2021).

[59] National Meteorological Information Center, Specialized Meteorological Dataset for Building thermal Environment Analysis in china, China Architecture & Building Press, Beijing, China, 2005, pp. 10–18.

[60] K. Chen, Design and Analysis of Experiments, second ed., Tsinghua University Press, Beijing, China, 2005, pp. 108–110.

[61] J. Tang, G. Gong, H. Su, F. Wu, C. Herman, Performance evaluation of a novel method of frost prevention and retardation for air source heat pumps using the orthogonal experiment design method, Appl. Energy 169 (2016) 696–708.

[62] Y. Pan, Building Energy Simulation Handbook, China Architecture & Building Press, Beijing, China, 2013, pp. 55–60.

[63] M.K. Urbikain, M.G. Davies, A frequency domain estimation of wall conduction transfer function coefficients, Energy Build. 51 (2012) 191–202.

[64] U.S. Department of Energy, EnergyPlus™ Version 8.7 Documentation Input Output Reference, 2016.

[65] D.B. Crawley, L.K. Lawrie, F.C. Winkelmann, W.F. Buhl, Y.J. Huang, C.O. Pedersen, R.K. Strand, R.J. Liesen, D.E. Fisher, M.J. Witte, J. Glazer, EnergyPlus: creating a new-generation building energy simulation program, Energy Build. 33 (4) (2001) 319–331.

[66] EnergyPlus 8.5 Manual, Lawrence Berkeley National Laboratory, USA, 2016.

[67] Ministry of Housing and Urban-Rural Development of the People's republic of China, Standard of Test Methods for thermal Environment of Building (JGJ/T347-2014), China Architecture & Building Press, Beijing, China, 2014.

[68] C. Wang, S. Deng, J. Niu, E. Long, A numerical study on optimizing the designs of applying PCMs to a disaster-relief prefabricated temporary-house (PTH) to improve its summer daytime indoor thermal environment, Energy 181 (2019) 239–249.

[69] C. Amaral, T. Silva, F. Mohseni, J.S. Amaral, V.S. Amaral, Experimental and numerical analysis of the thermal performance of polyurethane foams panels incorporating phase change material, Energy 216 (2021), 119213.

[70] R.H. Inman, H.T.C. Pedro, C.F.M. Coimbra, Solar forecasting methods for renewable energy integration, Prog. Energy Combust. Sci. 39 (6) (2013) 535–576.

[71] ASHRAE, Guideline 14-2014, Measurement of Energy and Demand Savings, Atlanta, 2014, pp. 17–20.

[72] ASHRAE, ASHRAE Handbook Fundamentals, American society of heating, Refrigerating and Air-Conditioning Engineers Inc., Atlanta, GA, 2013.

[73] ASHRAE, ANSI/ASHRAE standard 55-2013, in: Thermal Environmental Conditions for Human Occupancy, 2013.

[74] J. Zhao, Y. Du, Multi-objective optimization design for windows and shading configuration considering energy consumption and thermal comfort: a case study for office building in different climatic regions of China, Sol. Energy 206 (2020) 997–1017.

[75] Z. Zhou, S. Zhang, C. Wang, J. Zuo, Q. He, R. Rameezdeen, Achieving energy efficient buildings via retrofitting of existing buildings: a case study, J. Clean. Prod. 112 (2016) 3605–3615.

[76] M.E. Kohansal, H.R. Akaf, J. Gholami, S. Moshari, Investigating the simultaneous effects of building orientation and thermal insulation on heating and cooling loads in different climate zones, Architect. Eng. Des. Manag. 2021 (2021) 1–24.

[77] W. Hu, Y. Xia, F. Li, H. Yu, C. Hou, X. Meng, Effect of the filling position and filling rate of the insulation material on the insulation performance of the hollow block, Case Stud. Therm. Eng. 26 (2021) 101023.

[78] X. Li, S. Zheng, G. Tian, L. Zhang, W. Yao, A new energy saving ventilation system assisted by transpired solar air collectors for primary and secondary school classrooms in winter, Build. Environ. 177 (2020), 106895.

[79] S. Somasundaram, A. Chong, Z. Wei, S.R. Thangavelu, Energy saving potential of low-e coating based retrofit double glazing for tropical climate, Energy Build. 206 (2020), 109570.

[80] E. Cuce, Role of airtightness in energy loss from windows: experimental results from in-situ tests, Energy Build. 139 (2017) 449–455.

[81] M. Dabbagh, M. Krarti, Experimental evaluation of the performance for switchable insulated shading systems, Energy Build. 256 (2022), 111753.

[82] F. Chi, R. Wang, Y. Wang, Integration of passive double-heating and double-cooling system into residential buildings (China) for energy saving, Sol. Energy 225 (2021) 1026–1047.

[83] R. Narayanan, P. Parthkumar, R. Pippia, Solar energy utilisation in Australian homes: a case study, Case Stud. Therm. Eng. 28 (2021), 101603.